POLITECNICO DI TORINO

Master's Degree in Physics of Complex Systems

Master's Degree Thesis

Network approach to Circular Economy: heavy metals and plastic cycle accumulation analysis

Supervisors

Prof. Stefano BATTISTON

Prof. Luca DALL'ASTA

Candidate

Giulio GALFRÉ

October 2022

Abstract

In the last decade, *Circular Economy* has gained importance as the way to minimize emissions and consumption of raw materials. It is strongly based on sharing, reusing, repairing and recycling. Indeed, it represents a key value for *Sustainable Transition* since our planet can count on finite resources and circularity implies that materials can undergo the same processes many times (e.g. production, disposal, triage). However, some harmful compounds may accumulate in the soil, in the hydrosphere or even in human bodies during these cycles. In the literature, this issue has never been developed with a *Complex Network* approach. The aim of this thesis is to investigate how this could be done. The main objectives are (i) to develop a simplified network model of a circular economy whose nodes represent production or consumption stages, (ii) to test if and where such harmful compounds accumulate at different nodes in the network and (iii) to check whether this accumulation is robust under random perturbations on the network. Further, two applications are provided: heavy metals and plastic cycle. Based on the available literature, data from public agencies and suitable estimations, the model shows in both cases evidence of accumulation that is even robust under certain conditions.

Keywords: Network modelling, Heavy metals, Plastic, Circular Economy, Sustainable Transition, Complex network.

Summary

Introduction and aim of the thesis

Many solutions have been proposed to enforce the *Sustainable Transition*. One of them, *Circular Economy* has gained importance as the way to cut waste production, minimize emissions and consumption of raw materials. It is based on sharing, reusing, repairing and recycling. Circularity implies that materials can undergo the same processes many times (e.g. production, disposal, triage). However, some harmful compounds may accumulate in the soil, in the hydrosphere or even in human bodies during these cycles. In the literature, this issue has never been developed with a complex network approach.

The aim of this thesis is to investigate how this could be done. The main objectives are **(i) to develop a simplified network model of a circular economy whose nodes represent production or consumption stages, (ii) to test if and where such harmful compounds accumulate at different nodes in the network and (iii) to check whether this accumulation is robust under random perturbations on the network.**

As an application of this new perspective, the heavy metals and plastic cycles are investigated based on available data from local studies and public agencies.

Methodology

Thinking to Circular Economy, the relevant production or consumption stages of the cycle can be modelled as the *vertices* of a network. The *edges* can represent all the material flows between different stages of production, disposal, triage. The volume of those flows can be expressed by the *weight matrix*. Such a network can be described by the graph $\mathcal{G} = (V, E, \boldsymbol{W})$, where V represents the node set, E the edge set and $\boldsymbol{W}$ the weight matrix. Calling $\boldsymbol{P}$ the *stochastic matrix* obtained by simple normalisation of $\boldsymbol{W}$ and defining $\boldsymbol{x}(t) \in \mathbb{R}^{|V|}$ as the vector whose elements represent the mass stored at each node, assuming *mass conservation* and *linear-flow hypothesis* apply, the dynamics is described by the following equation

$$\boldsymbol{x}(t+1) = \boldsymbol{P}'\boldsymbol{x}(t). \tag{1}$$

In order to assess whether accumulation occurs, a simple measure is performed. First, it is set the initial condition to be $\boldsymbol{x}(t = 0) = \mathbf{1}$, where $\mathbf{1}$ corresponds to all-ones vector. Then the initial condition is applied to equation 1, namely $\boldsymbol{x}(t = 1) = \boldsymbol{P}'\boldsymbol{x}(t = 0) = \boldsymbol{P}'\mathbf{1}$. Finally, the net accumulation is evaluated as $\boldsymbol{\Delta} = \boldsymbol{x}(t = 1) - \boldsymbol{x}(t = 0)$. The accumulation occurs at all nodes $i \in V$ such that

$$\Delta_i = x_i(t = 1) - x_i(t = 0) > 0.$$

The condition $\Delta_i = 0$ defines the *accumulation threshold*.

Another measure of interest is $\bar{\boldsymbol{x}}$, the fixed point of 1, referred as the *equilibrium mass distribution*. This vector is such that $\bar{\boldsymbol{x}} = \boldsymbol{P}'\bar{\boldsymbol{x}}$ and gives information about the long-term behaviour of the system, since it is possible to prove that

$$\lim_{t\to+\infty} \boldsymbol{x}(t) = \bar{\boldsymbol{x}}\mathbf{1}'\boldsymbol{x}(t = 0) \propto \bar{\boldsymbol{x}}.$$

The *robustness to accumulation test* is performed with a Monte Carlo approach to the matrix $\boldsymbol{P}$, that is randomly changed according to a truncated gaussian distribution. The simulation is repeated 10000 times along a 1000 steps path. Then the results are averaged on the 10000 realisations for each step.

Some Julia functions[1] have been developed specifically for evaluating the accumulation, the equilibrium mass distribution and the robustness of results.

Results

According to the available literature, two possible networks can be drawn for plastic (Hoellein et al. 2021)(Windsor et al. 2019) and heavy metal (Shi et al. 2018) cycle. Both representations are shown in Figure 1.

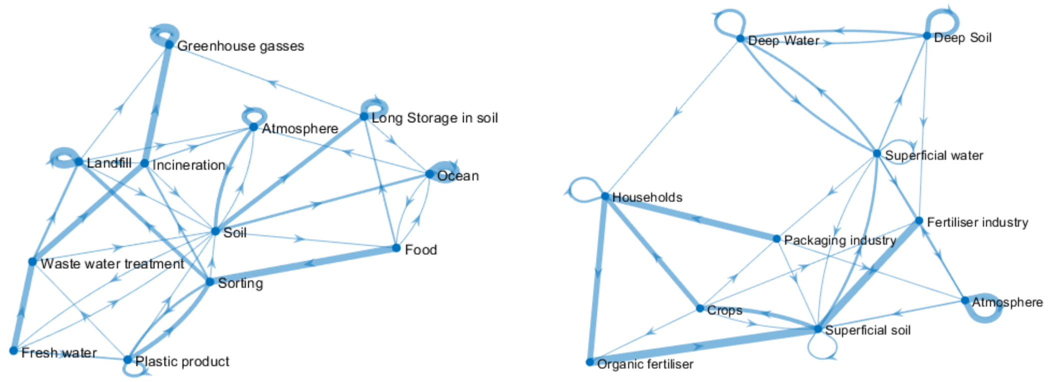

Figure 1: Graph representation of plastic (left) and heavy metals cycle (right).

For plastic, accumulation occurs at: Sorting facility, Landfill, Greenhouse gasses, Long storage in soil and Ocean vertices. Their net values respectively are: 0.290, 0.670, 0.870, 0.500 and 0.390. Since the graph has a sink, the equilibrium distribution coincides with a all-zeros vector with a 1 on the Atmosphere as Greenhouse gasses vertex. The accumulation appears to be robust in Landfill, in Soil (Figure 2), in Atmosphere, as Greenhouse gasses, in Long storage in soil and

[1] See `https://github.com/ggiulioo/Network_model_for_circular_economy`

in the Ocean.

For heavy metals, accumulation occurs at: Superficial soil, Superficial water and Households, with a net accumulation respectively of 1.58, 0.02 and 0.8. The equilibrium distribution shows that more than 70% of the mass tends to accumulate in Soil and Deep soil, Hydrosphere and Aquifer and Households. The accumulation in Soil appears to be very robust (Figure 2) while for Water and Atmosphere the results are not clear-cut: the mean value of simulations oscillates around the accumulation threshold. In Households, accumulation is robust even if it decreases after hundreds of changes.

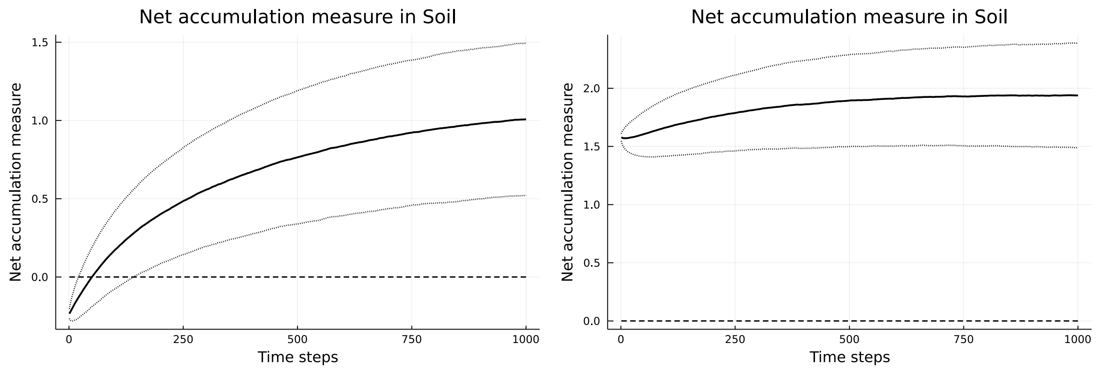

Figure 2: Robustness results for accumulation in Soil, respectively for plastic (left) and heavy metals (right). Solid lines represent mean values of simulations, dotted lines the mean values plus and minus the standard deviation and dashed line the net accumulation threshold.

Conclusion

The expected results are in great accordance with recent studies and observations available in the literature, both for plastic (Jamali et al. 2021)(Chenillat et al. 2021) and heavy metals (Baldantoni et al. 2010)(Gigliotti et al. 1996)(Jordao et al. 2006). In order to better estimate the accumulation rates, more data is needed both for heavy metals and plastic. Further research is necessary for estimating the volume of network flows. In general, a greater attention should be payed on the whole recycling process in order to prevent these and other potentially dangerous situations.

This work can be considered a starting point for analysing future scenarios with some set target (e.g. to increase recycled fraction of plastic, zero waste into landfill). With small changes and according to an energy function, some profitable stochastic paths can be followed change by change, with the purpose of exploring some real policies that can be adopted. Finally the best path can be selected from the bundle, once defined a suitable measure in term of economic cost.

Acknowledgements

I wish to show my appreciation to Prof. Stefano Battiston (University of Zurich) who inspired me with his great works on network and guided me throughout this project, ARPA Piemonte that kindly provided me the major part of local data and Mr. Irving Horne who helped me with the English language. I would also like to thank my friends and family who supported me and offered deep insight into the study.

"Omnia venenum sunt:
nec sine veneno quicquam existit.
Dosis sola facit, ut venenum non fit."
P. A. T. B. von Hohenheim (Paracelsus)

Table of Contents

List of Tables

List of Figures

Acronyms

HM

Heavy metal

EU

European Union

NMP

Nano- and micro-plastic

CS

Complex System

CE

Circular Economy

SDG

Sustainable Development Goal

n.a.

Value is not available

n.d.

Value is not determined or below the sensitivity of the instrument

LNFD

Linear Network Flow Dynamics

PC

Polycarbonate

PU

Polyurethane

PE

Polyethylene

PP

Polypropylene

PS

Polystyrene

PET

Polyethylene Terephthalate

PVC

Polyvinyl Chloride

ABS

Acrylonitrile-Butadiene-Styrene

PCL

Polycaprolactone

PHA

Polyhydroxyalkanoate

PHB

Polyhydroxybutyrate

PBS

Polybutylene succinate

PLA

Polylactic acid or polylactide

PMMA

Polymethyl methacrylate

Introduction

The interest in Complexity has increased exponentially since the beginning of the century. Many different fields have benefited from it, starting from Physics, Biology, Economics. And new challenges are rising. This huge buzz about Complexity was amplified by the Swedish Academy that awarded in 2021 the Italian physicist Giorgio Parisi with the Nobel Prize for his studies on interacting systems. Although a straightforward definition for Complex System (CS) does not exist, everyone has in mind what a CS is: when interacting elements of a huge set have a collective behaviour that is not immediately deductible from the behaviour of the single element, that is a CS. As the Nobel Prize physicist Paul Anderson stated in 1972, "More is different" (Anderson 1972). Basically, he argued that there are many phenomena in which the whole thing is more than the sum of all its components. Complexity is then characterised by other properties, such as *non-linearity*, *adaption*, *spontaneous order*. In few words, the reductionist hypothesis no longer applies. This is both an advantage and a disadvantage: non-linear systems can capture more general behaviours but suddenly their dynamics and stability become very hard to study.

Many contributions to this subject have been drawn from *Statistical Physics*, that is used to deal with huge amount of particles and agents. However one of the best available framework for studying CSs is indeed *Graph Theory* (Caldarelli 2020). Vertices represent the microscopic agents while edges their interactions.

According to Guido Caldarelli, a famous Italian physicist and CSs expert, networks are the most immediate tool to attempt a description of Complexity from below. Secondly, networks can model both structure and dynamics of lots of phenomena. Lastly, they allow a better visualization and it is possible to filter out unnecessary or irrelevant information (Caldarelli 2020). However, real CSs produce networks, usually called *Complex networks*, whose properties are topologically different both from random graphs and regular lattices. They are characterised by heavy-tails degree distribution, a high clustering coefficient and other connectivity properties among similar vertices that makes them difficult to artificially reproduce (Kim et al. 2008). In the last decade they have been employed for understanding big issues in Economics and Finance, such as: the structure of the control network of transnational corporations (Vitali et al. 2011), the contagion and systemic risk of financial institutions (Battiston, Caldarelli, et al. 2016)(Battiston, Farmer, et al. 2016)(Battiston, Puliga, et al. 2012) and the distribution of wealth and control across national markets (Glattfelder et al. 2013).

Thinking to our world, it has changed deeply in the last century. From the end of the Second World War, many microscopical "adjustments" led progressively to a more globalised and interconnected society. Technology supported this quick change by improving communication devices and providing new means of transports. If these new connections united together more and more people, markets and nations, new weaknesses appeared in this tangle of interactions. Social networks, markets, supply chains, diseases, economic crisis, environmental issues became strongly related to this new reality where the classical butterfly's flap located somewhere can change abruptly the global order of the system. This reminds the *phase transitions* that occur in Physics: once reached criticality, infinitely small perturbations can suddenly change the equilibrium of the system, resulting in a macro effect in terms of the order parameter. Many examples of that are before our eyes. In the last decades, we almost experienced the collapse of the world banking system in October 2008, after the outbreak of the Lehman crisis (Williams 2010). Furthermore, the Coronavirus disease 2019 (COVID-19), whose first case was identified in Wuhan in December 2019, quickly spread worldwide, resulting in a long-lasting pandemic (Page et al. 2021). In addition, the war in Ukraine, started in February 2022 (Makuch et al. 2022), made more evident how supply chains reward convenience instead of robustness.

This should draw attention on some ethical issues. The global population is still growing (Figure 3) and this "small change-big effect" pattern may increasingly affect our habits and everyday life. In fact, some personal behaviours can damage the smallest community, up to the global population. At this purpose, Caldarelli suggests some examples (Caldarelli 2010). The vaccination during a pandemic: is the individual will not to get vaccinated somehow more important than the health of frail members of the community? How long can we call this will "freedom"? And what does freedom mean in this super populated and connected world? Another example is about the massive fossil fuels use: is our freedom of movement more important than the human life on a Pacific island whose existence is strongly related to the sea level (therefore, to climate change) and whose inhabitants probably have never see a combustion engine?

These questions, especially the last one, allow us to understand how the environment is indeed a CS. For this reason, new and urgent policies have to be adopted in light of that. In fact, in order to avoid global crisis and to achieve some results to preserve human life on Earth and the environment as we know it, a change of pace is needed. The United Nations listed seventeen important targets, called Sustainable Development Goals (SDGs) (*Take Action for the Sustainable Development Goals* n.d.). These targets are a universal call to action to end poverty, protect the planet, and ensure that by 2030 all people enjoy peace and prosperity

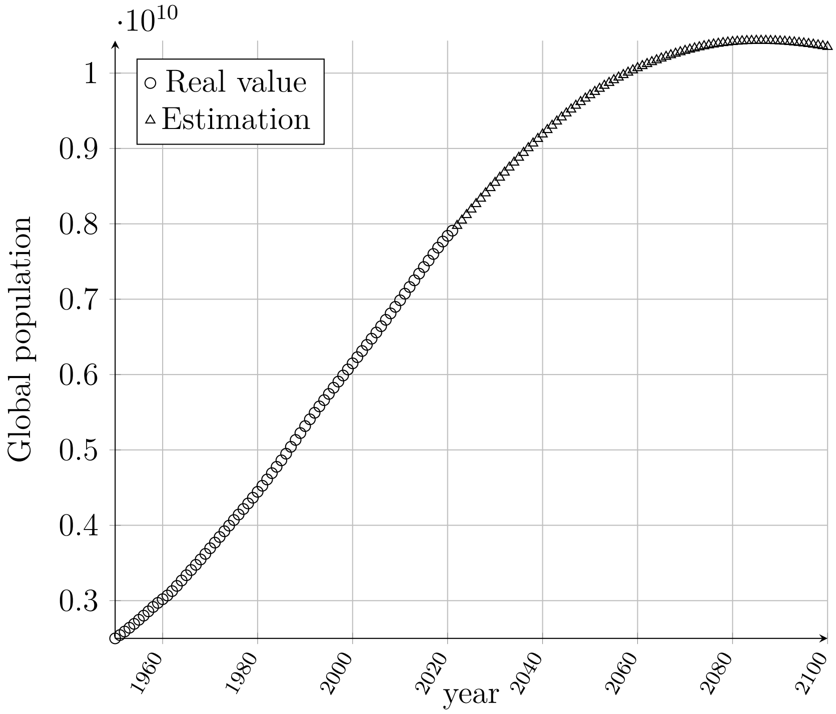

Figure 3: Global population: real values (1950-2021) and estimations (2021-2100)(Roser et al. 2013)

(UN 2022). However taking actions require good plans, since overnight measures can generate huge shocks to the economic system and society. For this reason policy makers need accurate descriptive and predictive models, in order to measure the impacts of different policies on our complex world.

Complex networks, Agent-based models and Diffusive models have been largely used for modelling Sustainability Transition (Tran 2014) and to understand how much this transition can be considered a risk or an opportunity for investors and markets (Battiston, Monasterolo, et al. 2021). However, due to confidentiality issues, many microscopic agent-to-agent data are not always available (Battiston, Farmer, et al. 2016). As a result, only some coarse grained analyses can be performed, based on real data belonging to large databases, e.g. EXIOBASE (Stadler et al. 2018). The loss of microscopic information in a model (induced or volunteer, depending on the availability or precision required) could increase the uncertainty on the long term outcomes (Tran 2014). Tran suggests a simple example to better clarify this point: a short-term efficiency improvement in a traditional vehicle may lead to long-term effects in vehicle market since, due to that, traditional motors could win the competition with alternative fuel ones (Tran 2014). This is one among the biggest issues to take into account when shaping a model.

Aim of the thesis

Many solutions have been proposed to enforce the Sustainable Transition and the achievement of different SDGs. One of them, Circular Economy (CE) has gained importance as the way to cut waste production, minimize emissions and consumption of raw materials. It is based on sharing, reusing, repairing and recycling. More generally, it is involved in the achievement of many different SDGs, such as Goal 12 (Responsible consumption and production), Goal 7 (Affordable and clean energy) and Goal 14 (Life below water). Circularity implies that materials can undergo the same processes many times (e.g. production, disposal, triage). However, some harmful compounds may accumulate in the soil, in the hydrosphere or even in human bodies during these cycles.

In literature, this issue has never been developed with a complex network approach. The aim of this thesis is to investigate how this could be done. The main objectives are (i) to develop a simplified network model of a circular economy whose nodes represent production or consumption stages, (ii) to test if and where such harmful compounds accumulate at different nodes in the network and (iii) to check whether this accumulation is robust under random or targeted perturbations on the network.

As an application of this new perspective, the heavy metals (HMs) and plastic cycles are investigated, based on available data.

Chapter 1

Network approach to Circular Economy: models and methods.

In this chapter the focus is entirely on how to build a suitable model for studying CE. A quick review on what has already been done and published in the literature is presented, especially for the two applications proposed, HMs and plastic. Then the attention moves towards the construction of a model based on *Linear Network Flow Dynamics* (LNFD) and some tools are provided in order to take advantages of this simplified framework. Lastly, some important issues about time and spatial scale, data availability and complexity are analysed in order to get more precise results from the model.

1.1 Review

A lot has been done in terms of research regarding HMs accumulation in soil (Shi et al. 2018). Several models have been developed using both real values (Nicholson et al. 2006)(Belon et al. 2012) and model estimations (Keller et al. 2001). Sometimes stochastic simulations have been performed for predicting future scenarios (Peng et al. 2016). However the main issue encountered by scientists is data availability in the short range interaction. Indeed, local conditions become fundamental and a great lack of data at this level remains the biggest source of uncertainty in all the models previously developed (Shi et al. 2018).

For plastic, the question is far more complicated since the full reconstruction of the cycle is still active matter of research: many aspects on degradation, nano-fragmentation as well as the final fate of plastic are still unclear (Koelmans et al. 2019, p. 27). In addition a general method for analysing nano-plastic in soil is missing (Koelmans et al. 2019, p. 33). Many studies have underlined the big amount of plastic, about 2.5×10^8 kg (Eriksen et al. 2014) in 2014, that wonders in the oceans and have analysed how it moves (Chenillat et al. 2021)(Jamali et al. 2021), but some recent studies (Hoellein et al. 2021)(Windsor et al. 2019) allow to pay greater attention to river catchments since they represent crucial points for plastic diffusion in the environment. Rivers represent the circulatory arteries of the water system on Earth and many agents interfere at this level. Even if precise data about flows, sources and sinks are still missing (Windsor et al. 2019), at this level, like a capillary, anthropogenic practises and natural phenomena blend together.

1.2 Linear network flow dynamics theory

The content of this section is largely influenced by *Lecture notes on Network Dynamics* (Como et al. 2021).

LNFD finds many applications in transport modelling, epidemiology, ecology, pharmacokinetics. In the literature (Jacquez et al. 1993), models based on LNFD are also known as *compartmental systems*.

Thinking to CE, the relevant production or consumption stages of the cycle can be modelled as the *vertices* of a network. While the *edges* can represent all the material flows between different stages of production, disposal, triage. The volume of those flows can be expressed by the *weight matrix*. Such a network can be described by the graph $\mathcal{G} = (V, E, \boldsymbol{W})$, where V represents the node set, E the edge set and $\boldsymbol{W}$ the weight matrix.

1.2.1 Notation

Before continuing with the dynamics, it is important to define $\mathbf{1}$ as the all-ones vector, $\mathbf{0}$ as the all-zeros vector, $\boldsymbol{d} := \boldsymbol{W}\mathbf{1}$ as the vector whose entries are the sum of the rows of $\boldsymbol{W}$, $\boldsymbol{D} := \text{diag}(\boldsymbol{d})$ a diagonal matrix whose diagonal entries are the elements of $\boldsymbol{d}$ and

$$\boldsymbol{P} := \boldsymbol{D}^{-1}\boldsymbol{W} \tag{1.1}$$

as the normalised weight matrix. By construction, this matrix is a *stochastic matrix*. This means that $\boldsymbol{P}\mathbf{1} = \mathbf{1}$, in other words, each row sum is equal to 1.

1.2.2 Mass conservation and Linear-flow hypothesis

Now calling $\boldsymbol{x}(t)$ the vector representing the mass distribution over vertices at time t, namely $x_i(t)$ represents the mass stored in vertex $i \in V$ at a given time t, the *mass conservation* implies that

$$x_i(t+1) = x_i(t) + \sum_{j\in V} f_{ji}(t) - \sum_{j\in V} f_{ij}(t), \tag{1.2}$$

where $f_{ij}(t)$ is the flow of mass from node i to node j. If $(i, j) \notin E$, $f_{ij} = 0$, for all $t \geq 0$.

The *linear-flow hypothesis* states that

$$f_{ij}(t) = \boldsymbol{P}_{ij} x_i(t). \tag{1.3}$$

This hypothesis applies whenever, at each time step, all the mass stored in a node i moves to its neighbourhood, according to matrix $\boldsymbol{P}$. This applies to the CE model since compounds addition or removing are not allowed. Note that the compounds storage can be modelled in the network by adding self-loops on corresponding nodes. By doing that, part of the mass is kept in the node.

Now, the combination of the *mass conservation* (1.2) with the *linear-flow hypothesis* (1.3) implies

$$\begin{aligned} x_i(t+1) &= x_i(t) + \sum_{j\in V} \boldsymbol{P}_{ji} x_j(t) - \sum_{j\in V} \boldsymbol{P}_{ij} x_i(t) && (1.4)\\ &= x_i(t) + \sum_{j\in V} \boldsymbol{P}_{ji} x_j(t) - x_i(t) \sum_{j\in V} \boldsymbol{P}_{ij} && (1.5)\\ &= x_i(t) + \sum_{j\in V} \boldsymbol{P}_{ji} x_j(t) - x_i(t) && (1.6)\\ &= \sum_{j\in V} \boldsymbol{P}_{ji} x_j(t) && (1.7) \end{aligned}$$

that is,

$$\boldsymbol{x}(t+1) = \boldsymbol{P}'\boldsymbol{x}(t). \tag{1.8}$$

1.2.3 Equilibrium

Equation (1.8) allows to study the dynamics and the equilibrium of the system. For studying some general properties of the network, it is important to recall the

Theorem 1.2.1 (Perron-Frobenius)**.** *Let $\boldsymbol{M}$ be a non-negative square matrix. Then, there exists a non-negative real eigenvalue $\lambda^\star \geq 0$ and non negative vectors $\boldsymbol{x} \neq \boldsymbol{0}$ and $\boldsymbol{y} \neq \boldsymbol{0}$ such that:*

(i) $\boldsymbol{M}\boldsymbol{y} = \lambda^\star \boldsymbol{y}$ and $\boldsymbol{M}'\boldsymbol{x} = \lambda^\star \boldsymbol{x}$;

(ii) $\max\left\{\omega_{min}, \omega^{-}_{min}\right\} \leq \lambda^{\star} \leq \min\left\{\omega_{max}, \omega^{-}_{max}\right\}$, *where*

$$\omega_{min} = \min_i \sum_j M_{ij}, \quad \omega^{-}_{min} = \min_j \sum_i M_{ij}$$

are the minimum row and column sum of $\boldsymbol{M}$*, while*

$$\omega_{max} = \max_i \sum_j M_{ij}, \quad \omega^{-}_{max} = \max_j \sum_i M_{ij}$$

are the maximum row and column sum of $\boldsymbol{M}$*;*

(iii) every eigenvalue λ *of* $\boldsymbol{M}$ *is such that* $|\lambda| \leq \lambda^{\star}$.

Proof. Let $\lambda \in \mathbb{C}$ be the eigenvalue of $\boldsymbol{M}$ with the maximum absolute value and $\boldsymbol{v} \in \mathbb{C}^n$ an associated eigenvector such that $\sum_i |v_i| = 1$. Let $\boldsymbol{z}$ be a vector such that $z_i = |v_i|$. Then,

$$|\lambda| z_i = |\lambda v_i| = |(\boldsymbol{Mv})_i| = \left|\sum_j M_{ij} v_j\right| \leq \sum_j |M_{ij}||v_j| = \sum_j |M_{ij}| z_j = (\boldsymbol{Mz})_i$$

for all i. This implies that the compact convex set

$$\mathcal{S} = \left\{\boldsymbol{x} \in \mathbb{R}^n_+ : \boldsymbol{1}'\boldsymbol{x} = 1, \boldsymbol{Mx} \geq |\lambda|\boldsymbol{x}\right\}$$

is non-empty. At this point, the proof separates.

(a) If $\boldsymbol{M}$ has at least one positive entry in each column ($\omega^{-}_{\min} > 0$),

$$\boldsymbol{1}'\boldsymbol{Mx} = \sum_j x_j \sum_i M_{ij} \geq \omega^{-}_{\min} > 0, \quad \forall \boldsymbol{x} \in \mathcal{S}$$

and the map $f : \mathcal{S} \to \mathbb{R}^n$ defined by

$$f(x) = \frac{\boldsymbol{Mx}}{\boldsymbol{1}'\boldsymbol{Mx}}, \quad x \in \mathcal{S},$$

is well defined and continuous on $\mathcal{S}$. Now it is time to show that $f(\mathcal{S}) \subseteq \mathcal{S}$. Consider an arbitrary vector $\boldsymbol{y} \in \mathcal{S}$, it is easily verified that

$$\boldsymbol{1}'f(\boldsymbol{y}) = \frac{\boldsymbol{1}'\boldsymbol{My}}{\boldsymbol{1}'\boldsymbol{My}} = 1.$$

Furthermore, since $\boldsymbol{M}$ is non-negative and $\boldsymbol{My} \geq |\lambda|\boldsymbol{y}$, it follows that

$$\boldsymbol{M}f(\boldsymbol{y}) = \frac{\boldsymbol{M}(\boldsymbol{Mz})}{\boldsymbol{1}'\boldsymbol{My}} \geq \frac{|\lambda|\boldsymbol{My}}{\boldsymbol{1}'\boldsymbol{My}} = |\lambda| f(\boldsymbol{y}),$$

that is $f(\boldsymbol{y}) \subseteq \mathcal{S}$. At this point, Brouwer's Theorem[1] guarantees that such a mapping admits at least one fixed points $\boldsymbol{x} = f(\boldsymbol{x})$ in $\mathcal{S} \subseteq \mathbb{R}^n_+$. In any fixed points $\boldsymbol{x}$, let $\lambda^\star = \boldsymbol{1}'\boldsymbol{Mx}$, then it follows that

$$\lambda^\star \boldsymbol{x} = \lambda^\star f(\boldsymbol{x}) = \boldsymbol{Mx},$$

so $\lambda^\star$ is an eigenvalue of $\boldsymbol{M}$ with associated eigenvector $\boldsymbol{x}$. Since $|\lambda|$ is the spectral radius, $\lambda^\star$ is an eigenvalue of $\boldsymbol{M}$ and $\boldsymbol{x} \in \mathcal{S}$,

$$|\lambda| \geq \lambda^\star = \boldsymbol{1}'\boldsymbol{Mx} \geq |\lambda|\boldsymbol{1}'\boldsymbol{x} = |\lambda|.$$

This means that $\lambda^\star = |\lambda|$ coincides with the spectral radius. Finally,

$$\lambda^\star = \sum_i \sum_j M_{ij} x_j = \sum_j \omega_j x_j \leq \omega^-_{\max},$$

and similarly, $\lambda^\star \geq \omega^-_{\min}$.

(b) If $\boldsymbol{M}$ contains some all-zero columns, they can be removed with the corresponding rows, ending with a matrix of dimension $k \times k$, $k < n$. If $k = 0$, $\lambda^\star = 0$ and $\boldsymbol{x} = \delta^{(i)}$, where i is the index of the all-zero columns. If $k \geq 1$, the point (i) applies to the smaller matrix of dimension $k \times k$. To complete the proof, notice that the arguments used above applies as well to the transpose matrix $\boldsymbol{M}'$, which has the same eigenvalues of $\boldsymbol{M}$.

■

In particular, more precise results hold true for stochastic matrices and it is possible to prove the

[1] See (Ben-El-Mechaieh et al. 2022)

Proposition 1.2.2. *Let $\mathcal{G}$ be a strongly connected graph and $\boldsymbol{P}$ its normalised weight matrix. Then, there exists a positive eigenvector $\bar{\boldsymbol{x}}$ such that*

$$\boldsymbol{P}'\bar{\boldsymbol{x}} = \bar{\boldsymbol{x}},$$

whose eigenvalue $\lambda = 1$ is geometrically and algebraically simple.

Proof. Suppose $\boldsymbol{x} \in \mathbb{C}^n$ is such that $\boldsymbol{P}\boldsymbol{x} = \boldsymbol{x}$. It follows that $\boldsymbol{P}|\boldsymbol{x}| \geq |\boldsymbol{P}\boldsymbol{x}| = |\boldsymbol{x}|$. Let $W := \operatorname{argmax}_i |x_i|$ and notice that, given $i \in W$,

$$|x|_i \leq \sum_j P_{ij}|x_j| \leq \sum_j P_{ij}|x_i| = |x_i|.$$

This implies that, for every j, such that $P_{ij} > 0$, $j \in W$. Since $\mathcal{G}$ is strongly connected, $V = W$ and so $|\boldsymbol{x}| = a\mathbf{1}$, with $a > 0$. It also follows that $\boldsymbol{P}|\boldsymbol{x}| = |\boldsymbol{x}|$ and similarly $|\boldsymbol{P}\boldsymbol{x}| = \boldsymbol{P}|\boldsymbol{x}|$. Furthermore for every node i

$$\left|\sum_j P_{ij}x_j\right| = \sum_j |P_{ij}x_j|,$$

that implies that there exists a unitary complex number z_i such that $x_j = az_i$, for every j in the neighborhood of i. The identity $\boldsymbol{P}\boldsymbol{x} = \boldsymbol{x}$ proves that $x_i = x_j$ for every j. Again if $\mathcal{G}$ is strongly connected, $\boldsymbol{x} = \alpha\mathbf{1}$ with $\alpha > 0$. This proves that $\lambda^\star = 1$ is geometrically stable. In order to show that is algebraically simple, the proof is by contradiction. Assume that is is not algebraically simple, in the Jordan canonical form of $\boldsymbol{P}$, it would show up a Jordan block of type

$$\boldsymbol{J} = \begin{pmatrix} 1 & 1 & 0 & \dots & \\ 0 & 1 & 1 & 0 & \\ & & \ddots & \ddots & \\ & \dots & 0 & 1 & 1 \\ & & \dots & 0 & 1 \end{pmatrix}$$

This leads to a contradiction as the off-diagonal of ones implies that $\boldsymbol{J}^t$ is not tending to zero any more and this can not happen because $\boldsymbol{P}$ is a stochastic matrix for all $t > 0$ and it remains bounded as t grows large. To prove the existence of the eigenvector $\boldsymbol{x} > \boldsymbol{0}$ of $\boldsymbol{P}'$ with relative eigenvalue equal to one, it is important to recall Theorem 1.2.1, that stated that it exists $\boldsymbol{x} \neq 0$, such that $\boldsymbol{P}'\boldsymbol{x} = \boldsymbol{x}$. Since $x_i = \sum_j P_{ij}x_i$, if $x_i = 0$, also $x_j = 0$ for each j in the out neighborhood of i. But again, a strongly connected graph like $\mathcal{G}$, would require $\boldsymbol{x} = \boldsymbol{0}$ that leads to a contradiction. ■

Furthermore, an asymptotic behaviour can be addressed for $\boldsymbol{x}(t)$. In fact, requiring the graph to be aperiodic, one can prove the following

Theorem 1.2.3. *If $\mathcal{G}$ is strongly connected and aperiodic, $\boldsymbol{P}'\bar{\boldsymbol{x}} = \bar{\boldsymbol{x}}$ and $\boldsymbol{x}(0) = \boldsymbol{x}_0$ then*

$$\lim_{t\to+\infty} \boldsymbol{x}(t) = \lim_{t\to+\infty} \boldsymbol{P}'^t\boldsymbol{x}_0 = \bar{\boldsymbol{x}}\boldsymbol{1}'\boldsymbol{x}_0.$$

Proof. The proof can be done proving that

$$\lim_{t\to+\infty} \boldsymbol{P}^t = \boldsymbol{1}\bar{\boldsymbol{x}}'$$

and then considering the transposed result

$$\lim_{t\to+\infty} \boldsymbol{P}'^t = \bar{\boldsymbol{x}}\boldsymbol{1}'.$$

Let $\boldsymbol{M} = \boldsymbol{P} - \boldsymbol{1}\bar{\boldsymbol{x}}'$, it follows from $\bar{\boldsymbol{x}} = \boldsymbol{P}'\bar{\boldsymbol{x}}$ and $\bar{\boldsymbol{x}}' = \bar{\boldsymbol{x}}'\boldsymbol{P}$ that

$$\boldsymbol{M}^t = \boldsymbol{P}^t - \boldsymbol{1}\bar{\boldsymbol{x}}'.$$

Note that by definition, $\boldsymbol{M}\boldsymbol{1} = \boldsymbol{P}\boldsymbol{1} - \boldsymbol{1}\bar{\boldsymbol{x}}'\boldsymbol{1} = 0$ and $\bar{\boldsymbol{x}}'\boldsymbol{M} = \bar{\boldsymbol{x}}'\boldsymbol{P} - \bar{\boldsymbol{x}}'\boldsymbol{1}\bar{\boldsymbol{x}}' = 0$. Now let's multiply the eigenvalue relation $\boldsymbol{M}\boldsymbol{x} = \lambda\boldsymbol{x}$, with $\lambda \neq 0$ and $\boldsymbol{x} \neq \boldsymbol{0}$, by $\bar{\boldsymbol{x}}'$ on the left, this means that

$$0 = \bar{\boldsymbol{x}}'\boldsymbol{M}\boldsymbol{x} = \lambda\bar{\boldsymbol{x}}'\boldsymbol{x},$$

hence $\bar{\boldsymbol{x}}'\boldsymbol{x} = 0$ and $\boldsymbol{P}\boldsymbol{x} = \boldsymbol{M}\boldsymbol{x} = \lambda\boldsymbol{x}$. But $\bar{\boldsymbol{x}}'\boldsymbol{x} = 0$ implies that $\boldsymbol{x} \neq \alpha\boldsymbol{1}$, with $\alpha \in \mathbb{R}$. From this, it follows that $\lambda \neq 1$. If $\mathcal{G}$ is strongly connected and aperiodic, this yields $|\lambda| < 1$. If a squared matrix $\boldsymbol{M}$ has a spectral radius strictly smaller than one, then

$$\lim_{t\to+\infty} \boldsymbol{M}^t = 0.$$

This can be proven very easily using matrix norm. As a result, recalling the definition of $\boldsymbol{M}$,

$$\lim_{t\to+\infty} \boldsymbol{P}^t = \mathbf{1}\bar{\boldsymbol{x}}'.$$

■

Theorem 1.2.3 states that the original mass tends to distribute according to $\bar{\boldsymbol{x}}$. For this reason $\bar{\boldsymbol{x}}$ is referred as *equilibrium mass distribution.* In other words, it gives information about long-term behaviour of the system. Since $\mathbf{1}'\boldsymbol{x}_0$ represents the total mass inserted at $t = 0$. Mass conservation implies indeed

$$\mathbf{1}'\boldsymbol{x}(t) = \mathbf{1}'\boldsymbol{x}_0, \quad \forall t > 0 \tag{1.9}$$

1.2.4 Accumulation measure

In this framework, the most immediate way to verify whether accumulation occurs is just checking one iteration of equation (1.8). In fact, setting the initial condition to $\boldsymbol{x}_0 = \mathbf{1}$ and considering

$$\boldsymbol{x}(t=1) = \boldsymbol{P}'\boldsymbol{x}_0 \tag{1.10}$$

$$= \boldsymbol{P}'\mathbf{1}, \tag{1.11}$$

the net accumulation is verified for all $i \in V$ such that

$$\Delta_i = x_i(t=1) - 1 > 0. \tag{1.12}$$

$\Delta_i = 0$ identifies the *accumulation threshold.*

Another measure of interest can be $\bar{\boldsymbol{x}}$ that allows to check how the mass is distributing along the network. This measure is immediate whenever the network has a sink or a sink component, since all the mass concentrates in that node or in that set of nodes. Otherwise it requires the evaluation of eigenvalues and eigenvectors of matrix $\boldsymbol{P}$.

1.3 Robustness test

With a Monte Carlo approach, the robustness to accumulation is verified. The method is based on slightly changing the non-zero entries of the normalised weight matrix $\boldsymbol{P}$. First, a non zero entry, $P_{ij}(t)$, is uniformly selected from the matrix $\boldsymbol{P}(t)$. Then a new value, $P_{ij}(t+1)$, is sampled from a truncated normal distribution whose mean value is equal to the original entry, $\mu = P_{ij}(t)$, and whose variance is directly proportional to the original entry multiplied by a variance factor constant for all entries and set to v_f:

$$\sigma^2 = P_{ij}(t)\, v_f.$$

With this approach, every entries have a different variance and bigger entries vary much more than smaller ones. At this point, the new value substitutes the previous entry and the matrix is normalised according to the change.

An accumulation measure is performed with the new matrix $\boldsymbol{P}(t+1)$ and the method is repeated 1000 time. This builds a path of changes in the matrix. The complete simulation is then repeated 10000 times and the average accumulation and its variance is evaluated at each step.

Some Julia functions[2] have been developed specifically for evaluating the accumulation, the equilibrium mass distribution and the robustness of results. A quick description of the code is available in section 1.5.

[2] See `https://github.com/ggiulioo/Network_model_for_circular_economy`

1.4 Problem formulation

Studying this kind of cycles, where many actors exchange material, can be difficult. The complexity of socio-economic system, data availability and time and spatial scale setting play an important role in defining the structure of the problem. In the following, each issue is discussed separately and different solutions are proposed for the two applications.

1.4.1 Time and spatial scale

Setting the time and the spatial scale is essential to capture the phenomenon without loosing or having too much information about short-range interaction and its evolution over time.

Regarding time scale, since accumulation can be studied over long period of time, as decades, and most human activities are strongly linked to the calendar year (e.g. agricultural practices), the time step chosen in this study is the year. It is important to stress that by doing this, a de-complexification is performed: all fluctuations in behaviours that occur in a time smaller than a year are flattened and just the mean value is considered.

As previously anticipated, in order to perform a consistent analysis, local data are required. But what does "local" mean? And how much information is available for constructing such a model? The reasoning done for time is no longer valid for space: people habits, agricultural practices, land morphology, climate, wealth and well-being of the population, may differ a lot from region to region (Shi et al. 2018). For this reason, the best choice for HMs is modelling a small environment, as a simplified unit (e.g. a small farm), with all its interaction with the environment and the outside world. While for plastic, the question is far more complicated since production, use and disposition can take place far away from each other. However, in order to achieve meaningful results valid for the regional scale, the model is chosen to be watershed-based, as proposed by Hoellein (Hoellein et al. 2021) and Windsor (Windsor et al. 2019). At this level, the main chain can be reconstructed.

All data presented in this paper are chosen to belong to the province of Turin (Italy). Whenever local data is not available, estimations are made in accordance with the available literature.

1.4.2 Data availability

Once selected the correct zoom in time and space (see subsection 1.4.1), many options are still available. Some studies (Donati et al. 2020) used EXIOBASE (Stadler et al. 2018) or similar databases for studying CE. This approach is too zoomed out for understanding what is really happening on the soil, in the hydrosphere or in human body. The input-output model and multi-regional databases can be useful for assessing macro cycles between nations but it does not have the correct resolution for analysing meso- and microscopic behaviours.

However, also the full reconstruction of the microscopic chain, where each family, production and consumption site are considered, can be problematic: it may require too effort. Then, at this level, one should deal with trade secrets, because basically all relationships between industries and suppliers are kept confidential. This is a big issue shared with financial modelling (Battiston, Farmer, et al. 2016).

In order to deal with these two issues, the LNFD model built for analysing CE, uses data from local studies and public authorities for both the applications and as much as possible. Data in this work are from Istituto Zooprofilattico Sperimentale del Piemonte, Liguria e Valle d'Aosta[3], Agenzia Regionale per la Protezione dell'Ambiente del Piemonte (ARPA)[4], Istituto Superiore per la Protezione e la

[3]See `https://www.izsplv.it/it/`

[4]See `http://www.arpa.piemonte.it/`

Ricerca Ambientale (ISPRA)[5]. This local data are an intermediate step between the two approaches described before: this allows to neglect all the small degrees of freedom but at the same time, saving the territoriality that characterises most of the interactions involved in a CE.

1.4.3 Complexity

The time and spatial scale together with the data resolution chosen in the previous sections, reduce the complexity of the socio-economic system. Fluctuations in time and space that usually characterise the production, the market and the behaviour of people, have been systematically flattened. The model presented is a coarse grained version of the CE network. However some general results and trend value can be assessed even within this simplified approach.

The role of fluctuations is considered with the Monte Carlo analysis described in subsection 1.3. In further research, it is possible to study how the network modifies itself over time to achieve some targets (e.g. zero plastic in landfill). This can be done fixing an energy function over network that reward (and accept) configurations whose "energy configuration" is lower than the previous one. Following that path may lead to some general strategies useful to investigate the intermediate steps and the cost of a specific CE policy.

1.5 Julia code for accumulation and robustness test

Some functions have been developed specifically for evaluating accumulation and robustness according to previous sections. The full Julia code, created by me, is

[5] See `https://www.isprambiente.gov.it/it`

available on GitHub here. In the following, the main functions are explained in terms of inputs and outputs.

1.5.1 Aanalysis

The function allows to detect the accumulation points in a graph, given the normalised weight matrix and a list with the name of all vertices. It gives as outputs the name of the vertices where the accumulation occurs and the net value of it, according to the methodology explained in the previous sections.

1.5.2 Mcanalysis

The function allows to do a single simulation of 1000 steps, given the the normalised weight matrix and a list with the name of all vertices. Optionally, the function can plot the accumulation along the single path.

1.5.3 MC

The function allows to perform a Monte Carlo analysis based on 10000 simulations, each one of 1000 steps, given the normalised weight matrix and a list with the name of all vertices. The final result consists on the averages and the standard deviations evaluated on all simulations at each step.

Chapter 2

Heavy metals cycle

In this chapter the HMs problem is formalised and a naive network model is presented for describing their accumulation in a small farm. Then an enlargement to this network is discussed, including external agents.

2.1 Introduction

In the following, a suitable definition and a list of most known sources of HMs are provided. Then their toxicity is discussed and some policies adopted by the European Union (EU) to prevent their accumulation and control their concentration are presented.

2.1.1 Definition

Thinking to HMs, there's a naive association to toxic and dangerous substances. This is because the term is general and misleading. A simple and unique definition for HMs doesn't exist (Duffus 2002). The word "heavy" suggests that weight and density play a great role in HMs identification. However there's no consistency in the literature in terms of density, since the lower bound for accepting a metal as HM is somewhere between 3.5 g/cm^3 and 7 g/cm^3(Duffus 2002). Although a

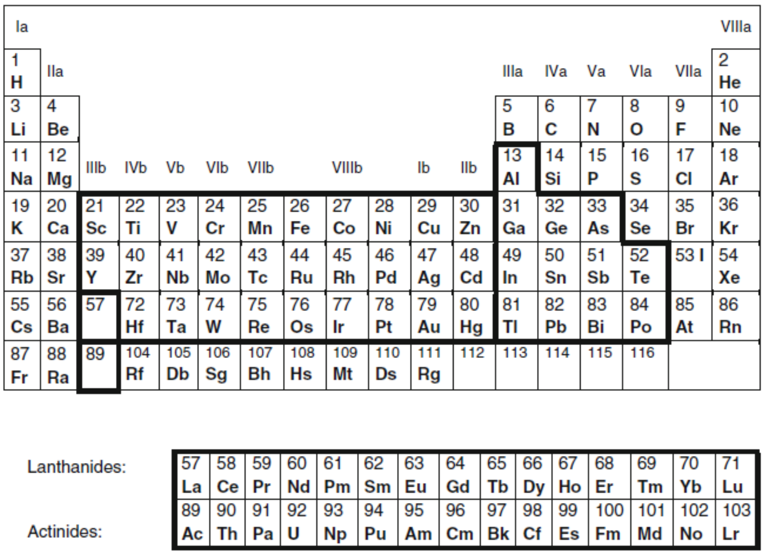

Figure 2.1: Periodic table of elements. Framed elements are candidate HMs according to (Appenroth 2010).

strict classification is not accepted by official Chemistry (Duffus 2002), the term is used to identify trace elements whose physical and chemical behaviour is similar to metals but they are quite relevant in Biology (Jaishankar et al. 2014). For example, for plants, metal density doesn't play any physiological or toxicological role (Appenroth 2010). Anyway some metals and their compounds are essential for plants biosynthesis, functioning of nucleic acids, growth, metabolism and stress resistance. They are Co, Cu, Fe, Mn, Mo, Ni and Zn and they are called micro-nutrients. Toxicity appears whenever certain concentration thresholds are overcome (Appenroth 2010). This is well observed in in-vivo experiments. However determining quantitatively the in-vivo dose-response relationship is quite difficult since changing HM in a particular site of a protein can alter completely the form and the function of the target protein. Additionally the complex interaction pattern of proteins doesn't allow to determine analytically if, and to what extent, a particular

HM is toxic (Appenroth 2010). Other HMs interacting with the ecosystem both directly and through compounds are Ag, Cd, Hg, Cr, Pb and As. In Figure 2.1, framed elements represent accepted HMs according to Appenroth (Appenroth 2010).

2.1.2 Main sources

HMs are regular constituents of Earth's crust but human activities have completely changed their spatial distribution in air, water and soil (Jaishankar et al. 2014). The main HMs sources are soil erosion, natural weathering of the Earth's crust, mining, industrial effluents, urban runoff, sewage discharge, insect or disease control agents applied to crops, and many others (Morais et al. 2012).

2.1.3 Toxicity

High concentration of HMs in soil can damage plants, animals and human. Their presence can seriously affect soil biodiversity and reduce plant growth (Ortiz et al. 2020). Due to their oxidation-reduction properties, they escape biological control mechanism disposed by organism and they bind to protein sites where they are not supposed to be, causing malfunctioning. This is the origin of toxicity. Dose and exposure time are fundamental to understand toxicity (Jaishankar et al. 2014). For example, in human, their intake can lower energy levels and damage functioning of the brain, lungs, kidney, liver, blood composition and other important organs. Long-term exposure can lead to gradually progressing physical, muscular, and neurological degenerative processes that imitate diseases such as multiple sclerosis, Parkinson's disease, Alzheimer's disease and muscular dystrophy. Repeated long-term exposure of some metals and their compounds may even cause cancer (Jarup 2003).

2.1.4 Latest surveys and present regulation

Since the beginning of the century, a lot has been done for reducing HMs concentration (Ortiz et al. 2020)(Velde, Boutron, et al. 2000b) and good results have been achieved all over the EU, as clearly visible in Figure 2.2.

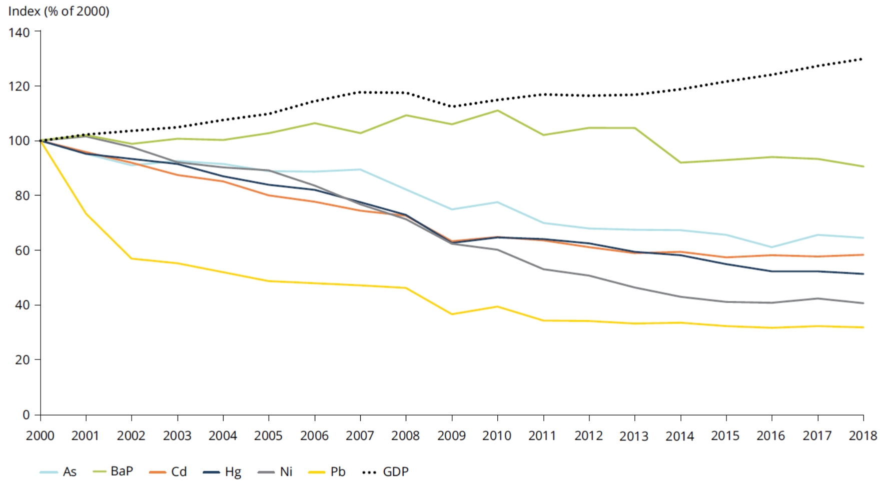

Figure 2.2: Development in EU-28 emissions, 2000-2018 (% of 2000 levels), of As, Cd, Ni, Pb, Hg and BaP. The EU-28 GDP appeared for comparison (Ortiz et al. 2020).

Italy, Germany and Poland were responsible together for around half of total EU emissions for Cd, Hg and Pb, but since 2005 Germany and Italy reduced their emissions of -11%, -48% and -31% and -49%, -48% and -33% respectively (*Heavy metal emissions in Europe* 2021).

A severe EU regulation has been promoted for limiting both emissions in air[1], water[2], soil[3] and presence in food[4] or compounds and devices[5]. Threshold values

[1]See Directive 2001/80/EC, Directive 2010/75/EU, Directive (EU) 2016/2284, Directive 2008/50/EC, Directive 2004/107/EC

[2]See Directive 2000/60/EC

[3]See Directive 86/278/EEC

[4]See Regulation (EC) No 1881/2006

[5]See Regulation (EC) No 1102/2008, Directive 2007/51/EC

and restrictions have been imposed whenever risks for environment or human health were assessed while target concentrations have been fixed for substances whose effects are active matter of research and risk has not been fully determined yet. Control agencies and standard criteria have been progressively set up[6] in order to better assess the concentrations in all the EU countries.

2.2 Network model and analysis

In order to address the problem of HMs accumulation, every possible sources of HMs have to be investigated and all exchanges between agents have to be analysed. According to other studies (Shi et al. 2018)(Keller et al. 2001), main players in HMs accumulation in soil are: industries, atmosphere and hydrosphere. Composting and fertilising in general are considered one of the most probable sources of HMs in soil (Shi et al. 2018). In fact the compost, both industrial and domestic, contains high level of HMs (Lopes et al. 2011).

At the same time, it is important to well estimate the flows that leave the soil. Up to now, only few studies are available and this represent one of the biggest source of uncertainty (Shi et al. 2018). All the adsorption mechanism of soil is difficult to take into account because it depends again on many local factors both physical and chemical (Dube et al. 2001). And this affects *surface runoff* and *leaching* (deep runoff) amounts, that together form the general *water runoff*.

Furthermore, there exists as well another source of uncertainty: the HMs out-flow due to harvest. This varies a lot from region to region since the plants uptake can be very different depending on the bio-availability of HMs, the amount of rainfall and even the soil morphology.

All these sources of uncertainty listed above are difficult to reduce. This is due

[6] See Regulation (EC) No 166/2006, Directive 2008/1/EC

to territoriality but also because HMs are trace elements and, as the name suggests, their concentration is very low (in general $\mathrm{ng\,kg^{-1}}$ of material). In many cases, it is difficult to spot anomalous concentrations, simply because their values can be easily confused with background values.

2.2.1 Naive farm model

Main agents

In order to study the accumulation and determine whether this can harm in some way human health or the environment, a simple model is presented. This naive approach try to consider the most important relationships between all the main HMs sources listed in the previous introduction. At the same time, the model takes into account all possible involvements between these sources and the environment. Therefore, a small farm is modelled and *Soil, Hydrosphere, Atmosphere, Crop and Organic fertiliser* are identified as the main agents in this early stage. Up to this point the farm can be indeed modelled as a *closed system* from an economic point of view: the only connections allowed with the outside world are mediated by Atmosphere and Hydrosphere. In this specific case, no external inorganic fertiliser is allowed and all contributions from specific industries (e.g. mining, packaging...) are accounted as part of air and water contaminants.

In the following, there is a representation of the model (Figure 2.3) where all players and their connections are shown with arrows. This model is inspired by Shi review (Shi et al. 2018), where many models are analysed and a summary outline is discussed. In this scheme, the Industries node is far more general than a single industry: it includes all the production sector and the market that lays outside the farm.

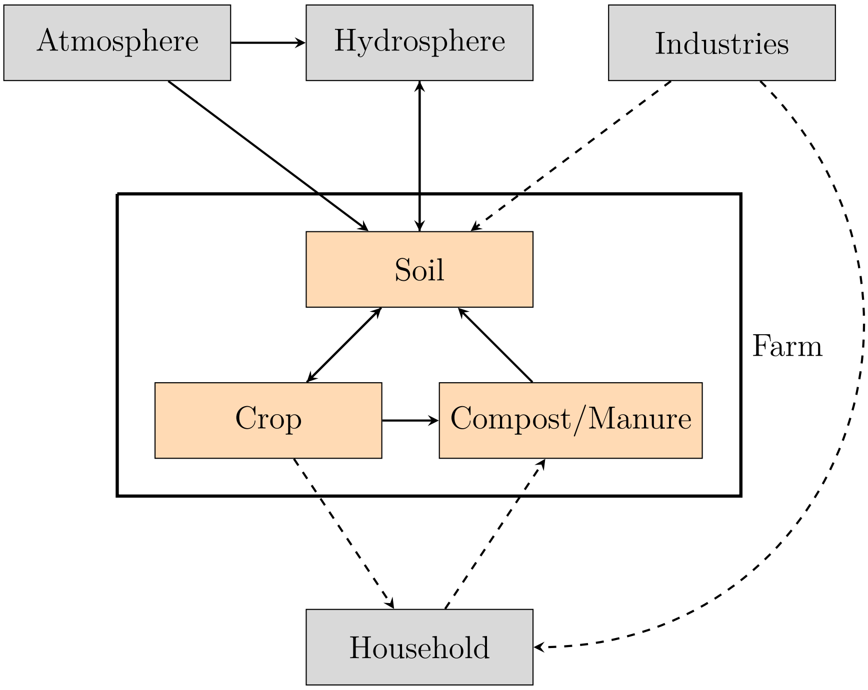

Figure 2.3: Interaction scheme for a small farm. Dashed arrows represent neglected interactions in the naive model.

Units

All flow rates are expressed in $\mathrm{g\,ha^{-1}\,y^{-1}}$. This choice allow much freedom in term of dimension of the farm since the area can be fixed a posteriori, if necessary .

Flows estimation

In the following, all data used in the model are ordered in tables. They are separated in Atmospheric deposition, Fertilisation, Irrigation, Leaching and Surface runoff (together Water runoff) and Crop harvesting.

(i) Atmospheric deposition is one of the biggest sources of soil poisoning especially where mines, iron and steel industry, thermal power plants, waste incineration, oil combustion plants are operating (Gerdol et al. 2000). Furthermore, this phenomenon could be more intensive if some barrier doesn't allow air circulation: this is the case of the Alps chain (Gerdol et al. 2000)(Velde, Boutron, et al. 2000a). In Table 2.1 are shown the atmospheric deposition rates collected from ARPA deposimeter in Piedmont (Badan 2012).

HM	Atmospheric deposition ($g\,ha^{-1}\,y^{-1}$)
Cd	2.6
Cr	11.2
Zn	396.2
Pb	37.1
Ni	21.3
Cu	49.0
As	4.2

Table 2.1: Atmospheric deposition rates from Arpa deposimeter (Badan 2012).

(ii) In this model, soil is fertilised only by compost or manure since industrial product such as inorganic fertiliser are not included in the naive model. According to The World Bank data (Database 2018b), in Italy it has been used, in 2018, $130\,kg\,ha^{-1}\,y^{-1}$ of fertiliser. ANPA made a report including information about trace elements in fertiliser (ANPA et al. 2001). Data are reported in table 2.2. Multiplying the concentration and the annual amount of fertiliser gives the rates in the correct units.

(iii) Irrigation need is estimated to be $5{,}000\,m^3 ha^{-1} y^{-1}$. This is the outcome of a simple count: the water used in Italy for agriculture (Rossi 2019), that is $1.17 \times 10^9\,m^3$ divided by the Italian irrigated area (Wriedt et al. 2008), 1.75×10^6 ha. Data on quality of water are taken from ARPA periodic survey (ARPA 2019). Then they are averaged on all rivers of the Turin province area and they are shown in table 2.3. Again a simple multiplication between water need per hectare and concentration gives the correct rates.

HM	Concentration in organic fertiliser ($mg\,kg^{-1}$)	Organic fertiliser rate ($g\,ha^{-1}\,y^{-1}$)
Cd	0.62	0.1
Cr	1.72	0.2
Zn	251.8	32.9
Pb	34.58	4.2
Ni	28.35	3.7
Cu	97.83	12.8
As	4.78	0.6

Table 2.2: HMs concentration in organic fertiliser (ANPA et al. 2001) and corresponding rates.

HM	Concentration in water ($mg\,L^{-1}$)	Irrigation rates ($g\,ha^{-1}\,y^{-1}$)
Cd	0.10	0.6
Cr	3.38	16.9
Zn	26.64	133.2
Pb	1.27	6.4
Ni	5.54	27.7
Cu	8.23	41.2
As	4.02	20.1

Table 2.3: HMs concentration in water, averaged on all Turin province rivers and corresponding rates.

(iv) As anticipated, leaching and surface runoff are very difficult to estimate. However between all estimations available in the literature, the worst case is chosen. This choice is intended to verify if some accumulation occurs, and if it is verified for the worst case, surely it will be always verified. Since it is an outflow from the soil, worst case means the greatest value. Total water runoff (Leaching and surface runoff) rates are shown in Table 2.4.

(v) Crop harvesting is again a quantity that need some clarification and some assumptions. In this model it is assumed that wheat cereals are cultivated, with an annual yielding rate of 5,265 $kg\,ha^{-1}\,y^{-1}$ (Database 2018a). In table 2.5 are shown all the concentrations of HMs in wheat cereals. In the same

HM	Water runoff ($g\,ha^{-1}\,y^{-1}$)
Cd	0.2
Cr	1.8
Zn	56.0
Pb	16.0
Ni	3.4
Cu	8.2
As	n.a.

Table 2.4: Water runoff corresponds to the sum of both surface runoff and leaching contribution. Data are taken from (Bonten et al. 2008)(Bengtsson et al. 2006)(Keller et al. 2001)

table are shown the rates, obtained by simple multiplication between the concentration and the annual yielding rate.

HM	Presence in wheat ($mg\,kg^{-1}$)	Crop rates ($mg\,kg^{-1}$)
Cd	0.04	0.2
Cr	n.a.	n.a.
Zn	57.69	313.4
Pb	0.02	0.1
Ni	0.66	3.6
Cu	4.25	23.1
As	n.a.	n.a.

Table 2.5: HMs concentration in wheat cereals (Brizio et al. 2016) and corresponding rates.

Network representation

In Figure 2.4 is shown the graph for the naive model. Some self-loops have been added on Soil, Hydrosphere and Atmosphere in order to mimic their retention. These values, expressed by percentage have been estimated using adsorption experiments (Sangiumsak et al. 2014)(Dube et al. 2001). In the following, all $\boldsymbol{W}$ and $\boldsymbol{P}$ matrices

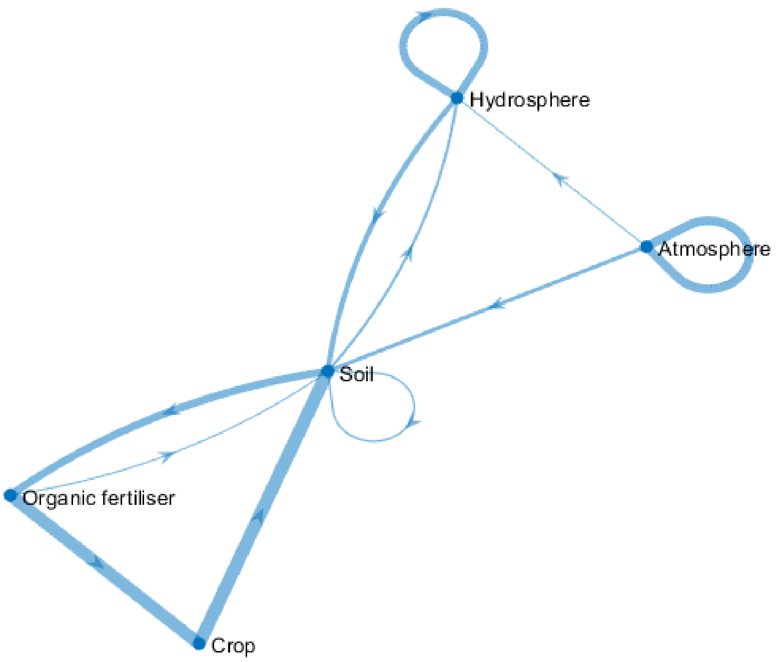

Figure 2.4: Graph representation of the farm model for HMs.

are listed for each HMs.

$$\boldsymbol{W}_{\text{Cd}} = \begin{pmatrix} 15\% & 0.2 & 0 & 0 & 0.2 \\ 0.6 & 60\% & 0 & 0 & 0 \\ 2.6 & 2\% & 68\% & 0 & 0 \\ 0.1 & 0 & 0 & 0 & 0 \\ 5\% & 0 & 0 & 0.1 & 0 \end{pmatrix}, \boldsymbol{P}_{\text{Cd}} = \begin{pmatrix} 0.150 & 0.425 & 0 & 0 & 0.425 \\ 0.400 & 0.600 & 0 & 0 & 0 \\ 0.300 & 0.020 & 0.680 & 0 & 0 \\ 1.000 & 0 & 0 & 0 & 0 \\ 0.050 & 0 & 0 & 0.950 & 0 \end{pmatrix} \tag{2.1}$$

$$\boldsymbol{W}_{\text{Cr}} = \begin{pmatrix} 15\% & 1.8 & 0 & 0 & 3.0^{*} \\ 16.9 & 60\% & 0 & 0 & 0 \\ 11.2 & 2\% & 68\% & 0 & 0 \\ 0.2 & 0 & 0 & 0 & 0 \\ 5\% & 0 & 0 & 0.2 & 0 \end{pmatrix}, \boldsymbol{P}_{\text{Cr}} = \begin{pmatrix} 0.150 & 0.319 & 0 & 0 & 0.531 \\ 0.400 & 0.600 & 0 & 0 & 0 \\ 0.300 & 0.020 & 0.680 & 0 & 0 \\ 1.000 & 0 & 0 & 0 & 0 \\ 0.050 & 0 & 0 & 0.950 & 0 \end{pmatrix} \tag{2.2}$$

$$\boldsymbol{W}_{\mathrm{Zn}} = \begin{pmatrix} 20\% & 56.0 & 0 & 0 & 313.4 \\ 133.2 & 60\% & 0 & 0 & 0 \\ 396.2 & 2\% & 68\% & 0 & 0 \\ 32.9 & 0 & 0 & 0 & 0 \\ 5\% & 0 & 0 & 32.9 & 0 \end{pmatrix}, \ \boldsymbol{P}_{\mathrm{Zn}} = \begin{pmatrix} 0.200 & 0.121 & 0 & 0 & 0.679 \\ 0.400 & 0.600 & 0 & 0 & 0 \\ 0.300 & 0.020 & 0.680 & 0 & 0 \\ 1.000 & 0 & 0 & 0 & 0 \\ 0.050 & 0 & 0 & 0.950 & 0 \end{pmatrix} \tag{2.3}$$

$$\boldsymbol{W}_{\mathrm{Pb}} = \begin{pmatrix} 15\% & 16.0 & 0 & 0 & 0.1 \\ 6.4 & 60\% & 0 & 0 & 0 \\ 37.1 & 2\% & 68\% & 0 & 0 \\ 4.2 & 0 & 0 & 0 & 0 \\ 5\% & 0 & 0 & 4.5 & 0 \end{pmatrix}, \ \boldsymbol{P}_{\mathrm{Pb}} = \begin{pmatrix} 0.150 & 0.845 & 0 & 0 & 0.005 \\ 0.400 & 0.600 & 0 & 0 & 0 \\ 0.300 & 0.020 & 0.680 & 0 & 0 \\ 1.000 & 0 & 0 & 0 & 0 \\ 0.050 & 0 & 0 & 0.950 & 0 \end{pmatrix} \tag{2.4}$$

$$\boldsymbol{W}_{\mathrm{Ni}} = \begin{pmatrix} 15\% & 3.4 & 0 & 0 & 3.6 \\ 27.7 & 60\% & 0 & 0 & 0 \\ 21.3 & 2\% & 68\% & 0 & 0 \\ 3.7 & 0 & 0 & 0 & 0 \\ 5\% & 0 & 0 & 3.7 & 0 \end{pmatrix}, \ \boldsymbol{P}_{\mathrm{Ni}} = \begin{pmatrix} 0.150 & 0.413 & 0 & 0 & 0.437 \\ 0.400 & 0.600 & 0 & 0 & 0 \\ 0.300 & 0.020 & 0.680 & 0 & 0 \\ 1.000 & 0 & 0 & 0 & 0 \\ 0.050 & 0 & 0 & 0.950 & 0 \end{pmatrix} \tag{2.5}$$

$$\boldsymbol{W}_{\mathrm{Cu}} = \begin{pmatrix} 15\% & 8.2 & 0 & 0 & 23.1 \\ 41.2 & 60\% & 0 & 0 & 0 \\ 49.0 & 2\% & 68\% & 0 & 0 \\ 12.8 & 0 & 0 & 0 & 0 \\ 5\% & 0 & 0 & 12.8 & 0 \end{pmatrix}, \ \boldsymbol{P}_{\mathrm{Cu}} = \begin{pmatrix} 0.150 & 0.210 & 0 & 0 & 0.590 \\ 0.400 & 0.600 & 0 & 0 & 0 \\ 0.300 & 0.020 & 0.680 & 0 & 0 \\ 1.000 & 0 & 0 & 0 & 0 \\ 0.050 & 0 & 0 & 0.950 & 0 \end{pmatrix} \tag{2.6}$$

$$\boldsymbol{W}_{\mathrm{As}} = \begin{pmatrix} 20\% & 0.1^{*} & 0 & 0 & 0.1^{*} \\ 20.1 & 60\% & 0 & 0 & 0 \\ 4.2 & 2\% & 68\% & 0 & 0 \\ 0.6 & 0 & 0 & 0 & 0 \\ 10\% & 0 & 0 & 0.6 & 0 \end{pmatrix}, \ \boldsymbol{P}_{\mathrm{As}} = \begin{pmatrix} 0.200 & 0.400 & 0 & 0 & 0.400 \\ 0.400 & 0.600 & 0 & 0 & 0 \\ 0.300 & 0.020 & 0.680 & 0 & 0 \\ 1.000 & 0 & 0 & 0 & 0 \\ 0.050 & 0 & 0 & 0.950 & 0 \end{pmatrix} \tag{2.7}$$

Network analysis

Accumulation results are shown in table 2.6. Although all normalised weight matrices $\boldsymbol{P}$ are very similar to each other, they have enough freedom to differentiate their results on accumulation. As clearly visible in the table, Soil is the common vertex for accumulation, with a net accumulation of 0.9 or more. This means that at each iteration (on the current time scale this corresponds to one year), the mass almost double. In other words, starting from a mass equal to $x_{\text{Soil}}(t) = 1$, after a step this will increase to $x_{\text{Soil}}(t+1) = 1.9$.

HM	**Net accumulation** $(\boldsymbol{x}(t=1) - \boldsymbol{x}(t=0))$	
	Location	Respective amount
Cd	Soil, Hydrosphere	0.90, 0.05
Cr	Soil	0.90
Zn	Soil	0.95
Pb	Soil, Hydrosphere	0.90, 0.46
Ni	Soil, Hydrosphere	0.90, 0.03
Cu	Soil	0.90
As	Soil, Hydrosphere	0.95, 0.02

Table 2.6: Accumulation results for HMs.

In table 2.7 are shown the mass distributions at equilibrium. Since Atmosphere has no in-flows, it represent a source, so the distribution has a zero in this vertex. This means that mass tends to be distributed in all other vertices. The accumulation measure and the mass distribution show that Soil and Hydrosphere are the most probable vertices for HMs accumulation. Note that for some HMs the mass distributions predict even higher concentrations in Hydrosphere than in Soil. However, on the long run, water meets a threshold in transporting HMs since HMs are in ionic form when found in water (Vargas-Solano et al. 2022), so their solubility plays an important role. Anyway this effect is not taken into account in this model. This would require a normalised weight matrix dependent on concentration, and by extension on time, and this is far beyond the scope of this simple model.

2.2.2 Enlarged model

This model represents an enlargement to the naive farm model presented in subsection 2.2.1. Some important external vertices are added, such as *Deep soil,*

	Vertices				
	Soil	Hydrosphere	Atmosphere	Crop	Fertiliser
$\bar{\boldsymbol{x}}_{\mathrm{Cd}}$	0.346	0.367	0	0.140	0.147
$\bar{\boldsymbol{x}}_{\mathrm{Cr}}$	0.353	0.282	0	0.178	0.187
$\bar{\boldsymbol{x}}_{\mathrm{Zn}}$	0.381	0.115	0	0.246	0.258
$\bar{\boldsymbol{x}}_{\mathrm{Pb}}$	0.320	0.677	0	0.001	0.002
$\bar{\boldsymbol{x}}_{\mathrm{Ni}}$	0.347	0.358	0	0.144	0.151
$\bar{\boldsymbol{x}}_{\mathrm{Cu}}$	0.366	0.201	0	0.213	0.220
$\bar{\boldsymbol{x}}_{\mathrm{As}}$	0.360	0.360	0	0.137	0.144

Table 2.7: Mass distribution for each HM.

Aquifer, Fertiliser/pesticides industry, Households and *Packaging industry.* These new vertices are thought to mimic the farm interaction with the outside world.

Deep soil represent the $0.3 - 10$m fraction of soil depth and it is separated from the superficial one, $0 - 0.3$m, called Soil for simplicity. A similar approach is developed for Hydrosphere, where the superficial water (rivers, runoffs...) is separated from the aquifer. This decision is made for taking into account different water-mediated processes that take place in soil.

Furthermore, two types of industry are added in order to take into account some external sources. In particular, packaging industry is considered for analysing all possible errors in sorting waste while composting at households. Finally, fertiliser/pesticides industry is needed for tracking another big source of HMs. Note that the connections between vertices are thought to be consistent even if precise data are not always available. For this reason and considering that all $\boldsymbol{P}$ are very similar to each other, a precise characterisation for each HM is abandoned. In this

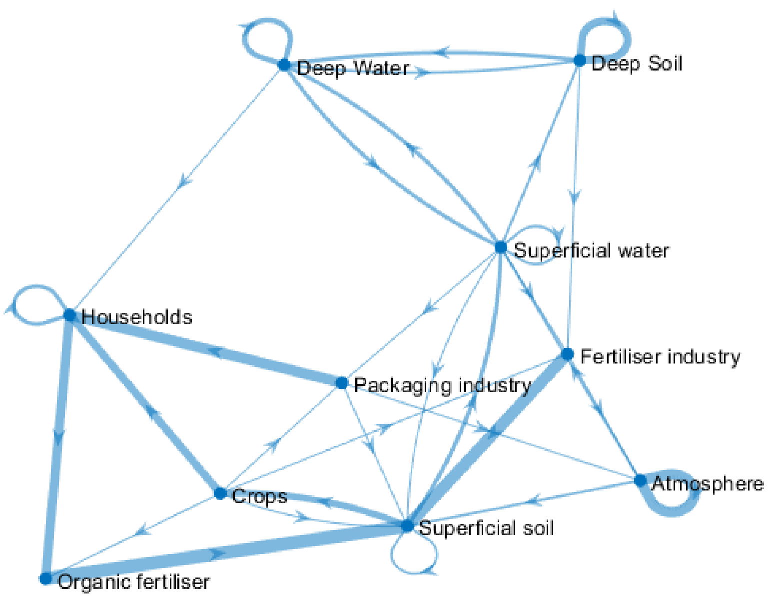

Figure 2.5: Graph representation of the enlarged model for HM.

framework a "mean" HM is considered and the corresponding $\boldsymbol{P}$ matrix is

$$\boldsymbol{P} = \begin{pmatrix} 0.180 & 0.320 & 0 & 0 & 0.500 & 0 & 0 & 0 & 0 & 0 \\ 0.200 & 0.200 & 0 & 0 & 0 & 0.200 & 0.300 & 0.050 & 0 & 0.050 \\ 0.300 & 0.020 & 0.680 & 0 & 0 & 0 & 0 & 0 & 0 & 0 \\ 1.000 & 0 & 0 & 0 & 0 & 0 & 0 & 0 & 0 & 0 \\ 0.050 & 0 & 0 & 0.100 & 0 & 0 & 0 & 0.100 & 0.650 & 0.100 \\ 0 & 0 & 0 & 0 & 0 & 0.600 & 0.300 & 0.100 & 0 & 0 \\ 0 & 0.300 & 0 & 0 & 0 & 0.200 & 0.400 & 0 & 0.100 & 0 \\ 0.900 & 0 & 0.100 & 0 & 0 & 0 & 0 & 0 & 0 & 0 \\ 0 & 0 & 0 & 0.700 & 0 & 0 & 0 & 0 & 0.300 & 0 \\ 0.100 & 0 & 0.100 & 0 & 0 & 0 & 0 & 0 & 0.800 & 0 \end{pmatrix} \tag{2.8}$$

In this specific case, the nodes where HM accumulates most are: Superficial soil, Superficial water and Households, with a net accumulation of $\Delta_{\text{Superficial soil}} = 1.58$, $\Delta_{\text{Superficial water}} = 0.02$ and $\Delta_{\text{Households}} = 0.8$. Again soil is an accumulation site with a mass more than doubled after a single iteration. Superficial water shows a weak accumulation, while in Households accumulation is more marked and this can be a problem because it can enter the humans food chain and bodies.

The equilibrium mass distribution is approximately

$$\bar{\boldsymbol{x}} = \begin{pmatrix} 0.196 & 0.133 & 0.029 & 0.098 & 0.097 & 0.130 & 0.130 & 0.036 & 0.127 & 0.024 \end{pmatrix}. \tag{2.9}$$

Note that, in this case, the Atmosphere has in-flows due to industries. For this reason the graph is fully connected and the mass distribution has no zero entries. The equilibrium distribution shows that more than 70% of the mass tends to accumulate in Superficial soil and Deep soil, Superficial water and Aquifer and Households.

The model predicts a very strong accumulation in soil. This seems to contradict the actual trend where HMs concentration in soil has decreased during the last decade as a consequence of the EU policies (see 2.1.4). However, the use of compost as soil amendment has been proved to be responsible of the unusual increasing of HMs availability in soil (Baldantoni et al. 2010)(Gigliotti et al. 1996)(Jordao et al. 2006) and this trend is confirmed by this model where one among the biggest source of HMs considered is organic fertiliser.

2.2.3 Robustness analysis

In the following the results of robustness test are shown in Figures 2.6, 2.7, 2.8, 2.9 and 2.10. The accumulation in Soil appears to be very robust while for Superficial water and Atmosphere the results are not clear-cut: the mean value of simulations oscillates around the accumulation threshold. Deep soil and water do not constitute a source of accumulation on average but it may occurs. In Households, accumulation is robust even if it decreases after hundreds of changes.

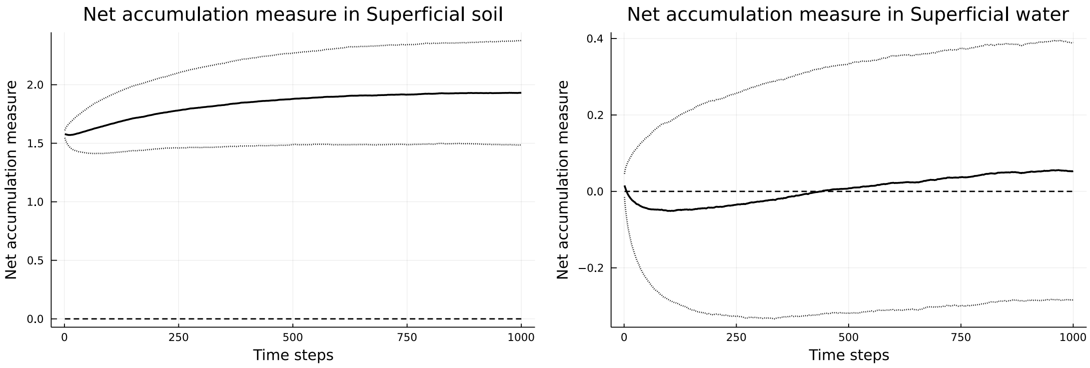

Figure 2.6: Robustness results for Superficial soil and Superficial water. Solid lines represent mean values of simulations, dotted lines the mean values plus and minus the standard deviation and dashed line the net accumulation threshold.

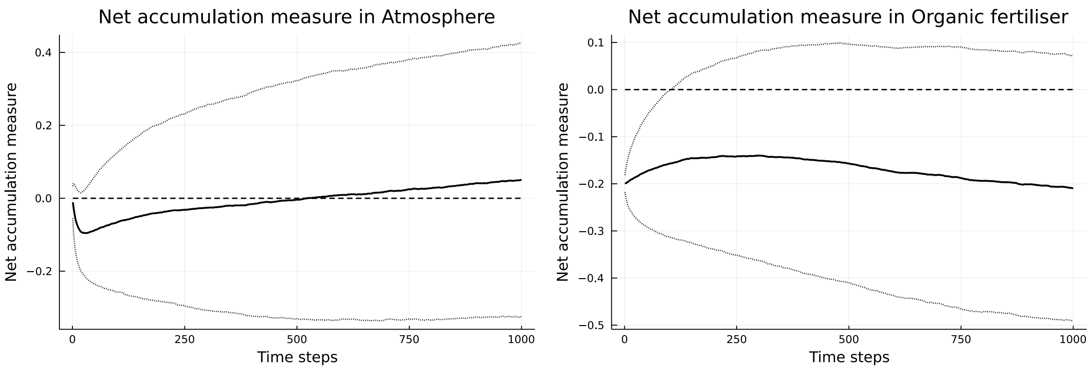

Figure 2.7: Robustness results for accumulation in Atmosphere and Organic fertiliser. Solid lines represent mean values of simulations, dotted lines the mean values plus and minus the standard deviation and dashed line the net accumulation threshold.

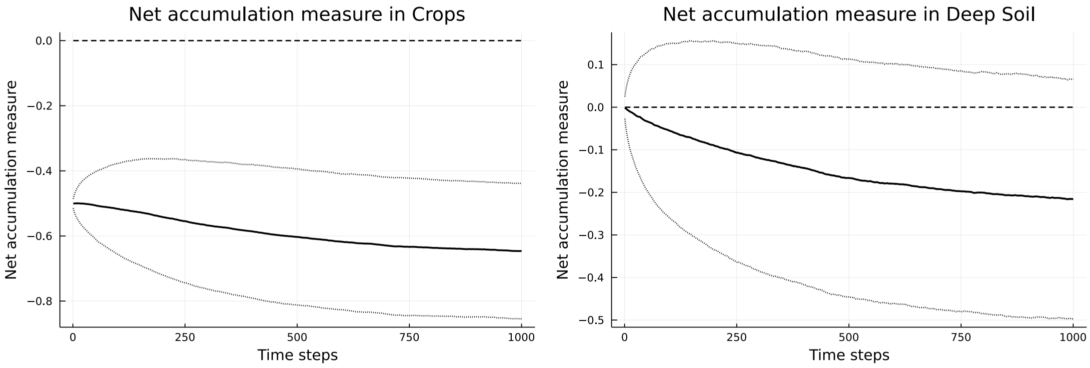

Figure 2.8: Robustness results for accumulation in Crop and Deep soil. Solid lines represent mean values of simulations, dotted lines the mean values plus and minus the standard deviation and dashed line the net accumulation threshold.

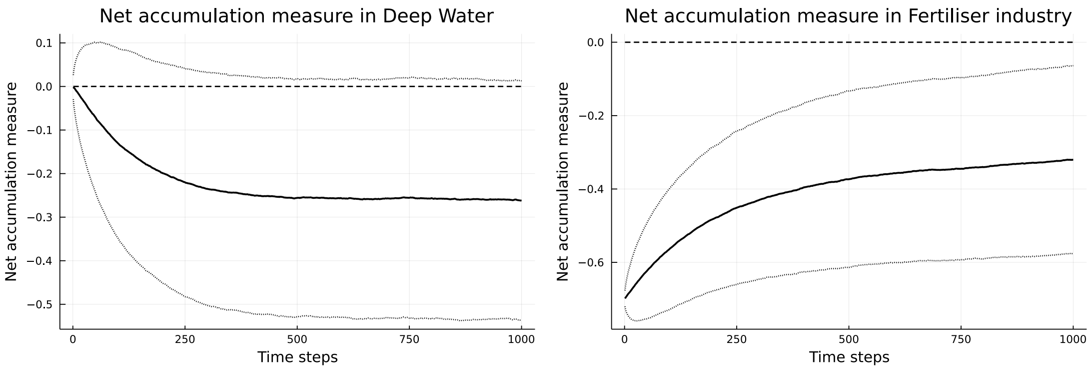

Figure 2.9: Robustness results for accumulation in Aquifer and Fertiliser/pesticides industry. Solid lines represent mean values of simulations, dotted lines the mean values plus and minus the standard deviation and dashed line the net accumulation threshold.

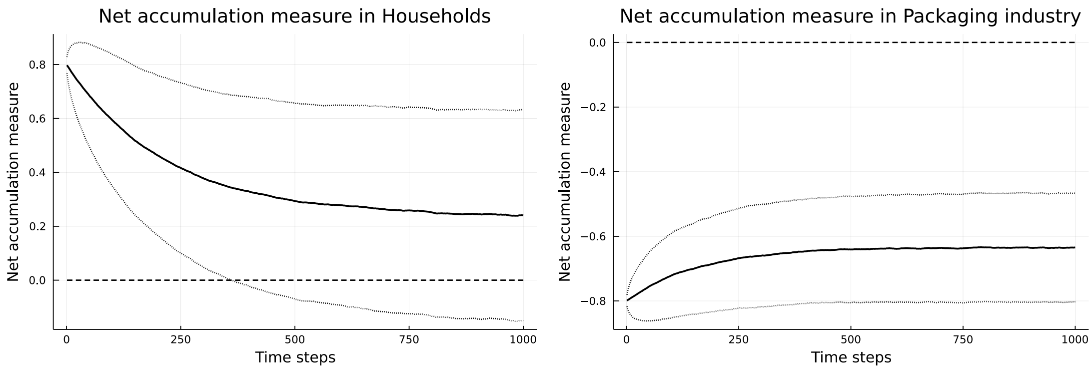

Figure 2.10: Robustness results for accumulation in Households and Packaging industry. Solid lines represent mean values of simulations, dotted lines the mean values plus and minus the standard deviation and dashed line the net accumulation threshold.

Chapter 3

Plastic cycle

In this chapter the plastic cycle is investigated. Conscious that there is still a huge lack of data and research, a quick introduction to the plastic problem is presented, then the network is built and tested with respect to accumulation. Lastly the robustness analysis is performed.

3.1 Introduction

3.1.1 Definition

Plastic is a "polymeric material that has the capability of being molded or shaped, usually by the application of heat and pressure. This property of plasticity, often found in combination with other special properties such as low density, low electrical conductivity, transparency, and toughness, allows plastics to be made into a great variety of products" (Rodriguez 2022).

Since its discovery, many types of plastic have been invented for fulfill industry requirements and needs. The most common ones, that accounts for more than 80% of European plastic demand (Gewert et al. 2015), are: Polycarbonate

(PC), Polyurethane (PU), Polyethylene (PE), Polypropylene (PP), Polystyrene (PS), Polyethylene Terephthalate (PETE or PET), Polyvinyl Chloride (PVC), Acrylonitrile-Butadiene-Styrene (ABS). Over one-third of plastic in Europe and United States is designed to be discarded within three years of their production (Gewert et al. 2015).

3.1.2 Production, presence and recycling

In twentieth century, after being a great opportunity in the period following the Second World War, plastic become a problem (Institute 2022). In early 1980s, plastic waste started worrying the planet since its production was still going on but, basically due to the same properties that made it popular (e.g durability), this material was hard to dispose of.

Furthermore, since it can't be easily destroyed by elements and biological activity, plastic starts wondering all around the planet, transported by rivers and wind (Jambeck et al. 2015). Nowadays it is so widespread that particles can be found even in areas with very little human influence, like deep sea, Arctic sea ice and glaciers (Windsor et al. 2019).

Some types of plastic can be easily recycled. This is the case of thermoplastics that can be re-melted and re-molded. While other ones, e.g. thermoset plastics, contain polymers that form irreversible chemical bonds and cannot be recycled. Examples of non-recyclable plastics include bioplastics, composite plastic, plastic-coated wrapping paper and polycarbonate.

However, recyclable plastic can not undergo the recycling process endlessly, because the increasing presence of impurities does not allow the material to regain the original properties. For this reason new matter must be combined with recycled material to have new plastics from the older one. Estimations show that 55% of plastic was directly discarded while only 9% was recycled in the period 1950-2015

(Ritchie et al. 2018). Discarded fraction reduced year by year compared with recycled fraction (Figure 3.2), but since plastic production is still increasing (Geyer et al. 2017) (Figure 3.1), the volume of plastic discarded is not decreasing at all.

In Figure 3.3 is shown the fate of the cumulative mass of plastic produced in the period 1950-2015 according to (Ritchie et al. 2018). In Figure 3.3, *Still in use* terminal represents all the plastic produced that is still having some function, including the plastic that has undergone the recycling process. *Recycled* node represents the plastic that has been sorted, melted and reused. Note that the final fate of recycled plastic follows the same pattern of *Total plastic production* fate: 60% of recycled plastic goes *To landfill*, versus 55% of the total plastic production, 20% *To incinerator* versus about 8.5% and 20% is still in use versus about 30%. This proves that the recycling mechanism delays the final disposal of plastic, rather than reducing the waste production.

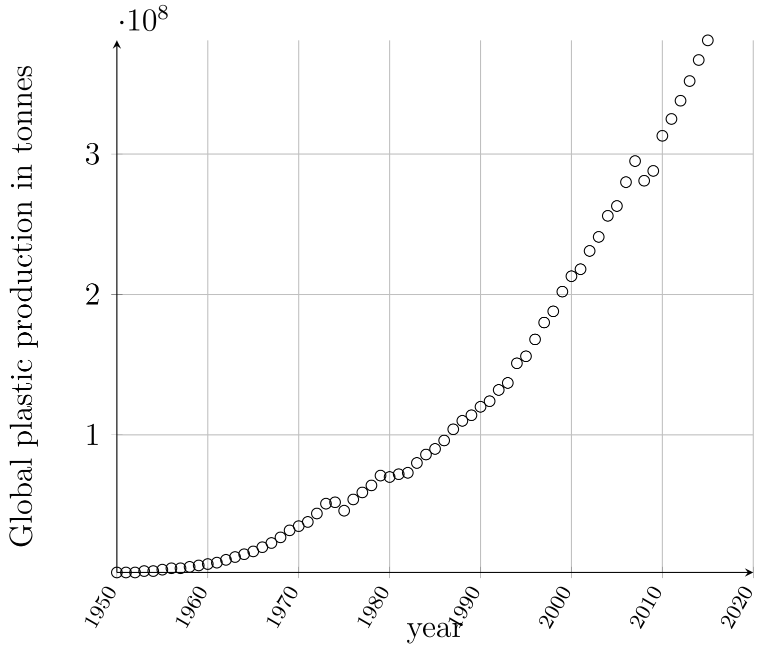

Figure 3.1: Global plastic production from 1950 to 2015 (Geyer et al. 2017)

In addition, risk assessment for plastic is not fully determined, since there are

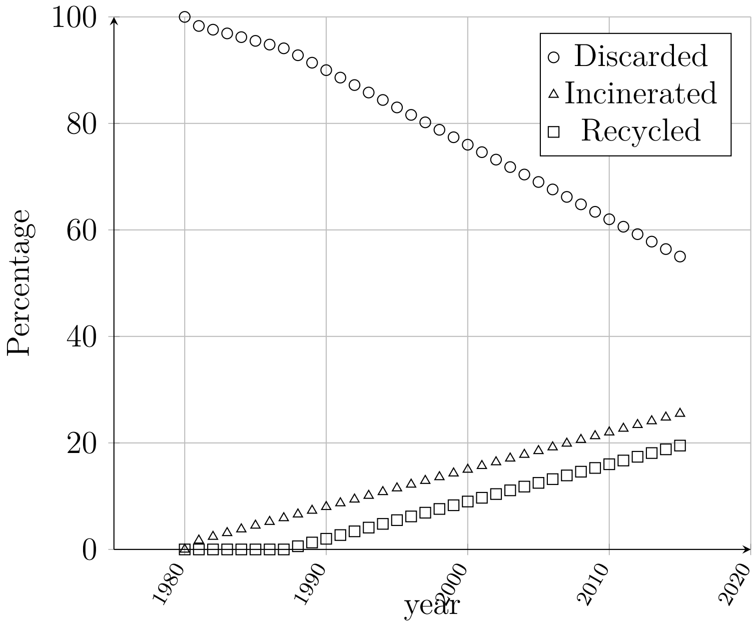

Figure 3.2: Estimated percentage of global plastic waste recycled, incinerated and discarded from 1950 to 2015 (Geyer et al. 2017)

gaps in knowledge on the process of fragmentation from micro- to nano-plastics and there is a complete lack of information about risks of nano-plastics both for humans and the environment (Koelmans et al. 2019).

3.1.3 Fate of plastic

When plastic is discarded in the environment, a very slow degradation path starts. First, the plastic is subjected to macro movements and breakage in smaller parts (mechanically), then the UV radiation or some thermal source can initiate the weakening and the fragmentation from macro- to micro- up to the nano-scale. While this disintegration is running, more and more surface is exposed to UV from the Sun and the process can increase its speed (Gewert et al. 2015). Later on, only for certain types of plastic, another phase can happen: biodegradation. This is basically a digestion phase where some enzymes, excreted by microbes

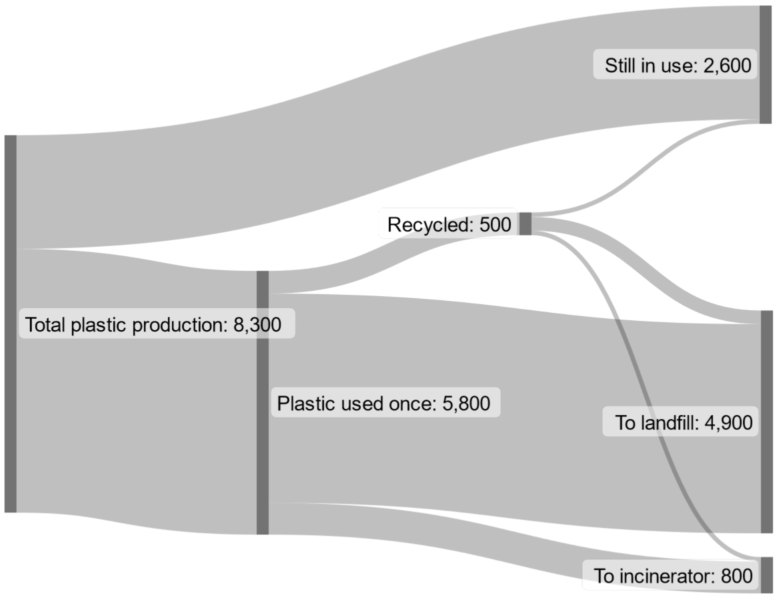

Figure 3.3: Cumulative mass of plastics over the period 1950-2015, measured in million tonnes (Ritchie et al. 2018). Flows sharing the same fate are indicated by the same colour and labels.

that colonized the surface of the debris, or various metabolic processes inside microbes, can degrade plastic polymer (Ahmed et al. 2018). The full digestion mechanism is available in Figure 3.4. The process can happen under aerobic conditions (the oxygen acts like an electron acceptor for the microbes) and the main products are CO_2 and H_2O and other metabolic products. Conversely, under anaerobic conditions (sulfate, nitrate, iron, carbon dioxide and manganese can act as electron acceptors), also CH_4 and other residues can be found (Ahmed et al. 2018). Hydrophobicity, presence of additives and enzymes characteristics are the control parameters of biodegradation (Ahmed et al. 2018). A list of specific enzymes and plastics compatible for degradation is shown in Table 3.1.

Type	Enzyme	Plastics
Bacteria		
	Lipase	PCL
	Unknown	PHB, PCL and PBS
	Lipase	PE, PBS and PCL
	Serine hydrolase	PHA
	Unknown	PET
	Unknown	PVC
Fungi		
	Glycosidase	PCL
	Unknown	PHB
	Catalase, protease	PCL
	Unknown	PHB and PCL
	Cutinase	PCL
	Manganese peroxidase	PLA and PE
	Serine hydrolase	PU

Table 3.1: Bacterial and fungi that can produce enzymes/strains involved in biodegradation of plastic (Ahmed et al. 2018).

3.1.4 Toxicity

In order to provide specific properties to plastic, some additives are added to the polymers (Gewert et al. 2015). These additives can be plasticizers, flame retardants, antioxidants, acid scavengers, light and heat stabilizers, lubricants, pigments, antistatic agents, slip compounds and thermal stabilizers (Hahladakis et al. 2018). However, since the major parts of these additives are not covalently bonded to polymer, they can leach out as plastic degrades and enter into the environment as persistent organic pollutants (POPs) (Stringer et al. 2001). Furthermore, plastic degradation itself leads to the release of intermediate and dangerous chemicals (Gewert et al. 2015), both solid and gaseous. Once initiated, plastic debris can in fact produce CH_4, C_2H_4, C_2H_6, C_3H_6 depending on the plastic type. Several experiments have been performed to assess more precise production rates and enhancing factors. Some results (Royer et al. 2018) are available in Table 3.2.

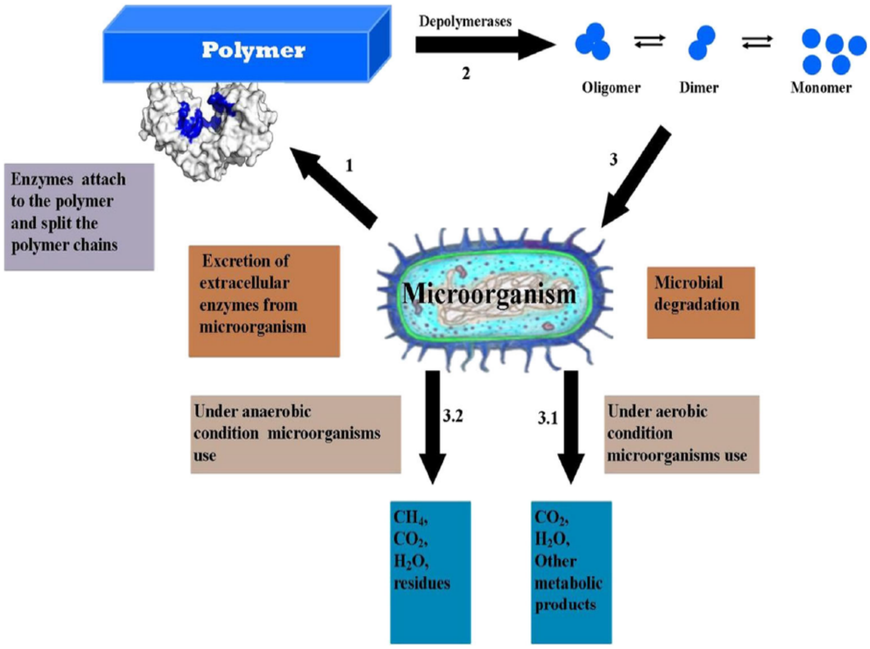

Figure 3.4: Biodegradation of plastic. General scheme for metabolic and enzymatic digestion mechanism (Ahmed et al. 2018).

To understand to what extent these emissions contribute to the greenhouse gasses balance, a simple calculation is proposed. Considering the worse case scenario, that is all the plastic produced until 2015, about 8.3×10^{15} g (Geyer et al. 2017), is composed only by the greater emitter. Based on Table 3.2, this corresponds to Low density PE, whose estimated methane production rate is $1.5 \times 10^{6}\,\mathrm{pmol\,g^{-1}\,y^{-1}}$ and whose molar weight is about $28\,\mathrm{g\,mol^{-1}}$. With some multiplications, the final methane emission due to the total plastic production up to 2015 is about $3.48 \times 10^{11}\,\mathrm{g\,y^{-1}}$. This quantity seems to be not so relevant if compared to $1.45 \times 10^{14}\,\mathrm{g\,y^{-1}}$, that represents the methane emission due to agriculture (Smith et al. 2021). However methane emission due to plastic degradation will continue potentially throughout the whole lifetime of object. Furthermore, the rate even increases in time due to the always greater surface available in degradation phase. This has been tested with material of different age and degradation path (Royer et al. 2018). The rates are shown in Figures 3.5 and 3.6 in case of new Low density PE and some pieces of the same material collected in the open ocean after an unknown residence time.

Plastic type	CH_4 (pmol g^{-1} d^{-1})		C_2H_4 (pmol g^{-1} d^{-1})	
	light	dark	light	dark
PC	10 ± 2	n.d.	24 ± 5	n.d.
PMMA	30 ± 3	n.d.	24 ± 1	20 ± 1
PP	170 ± 10	n.d.	50 ± 1	n.d.
PET	500 ± 20	50 ± 10	64 ± 11	n.d.
PS	730 ± 110	120 ± 30	910 ± 10	60 ± 5
High density PE	90 ± 10	n.d.	190 ± 20	n.d.
Low density PE	4100 ± 200	n.d.	5100 ± 400	n.d.

Table 3.2: Mean production rates of CH_4 and C_2H_4 from selected plastics debris in light and dark. Error represents the standard deviation of triplicate samples (Royer et al. 2018).

3.2 Network model and analysis

Data available for building the network

A great gap in knowledge lays beyond the precise determination of all possible flows between the main agents of plastic cycle. This limit has been widely recognised by the literature (Hoellein et al. 2021)(Windsor et al. 2019). However, based on some academic papers (Ritchie et al. 2018)(Geyer et al. 2017) and data from government agencies (OECD 2022)(Koelmans et al. 2019), some proportions in terms of flows have been addressed and flow volumes has been hypothesised. Further studies can not only better estimates these flows, but even add some important vertices that have been neglected or underestimated at present.

Main vertices have been identified according to (Windsor et al. 2019)(Hoellein et al. 2021)(Hahladakis et al. 2018). They are *Plastic products* or products with

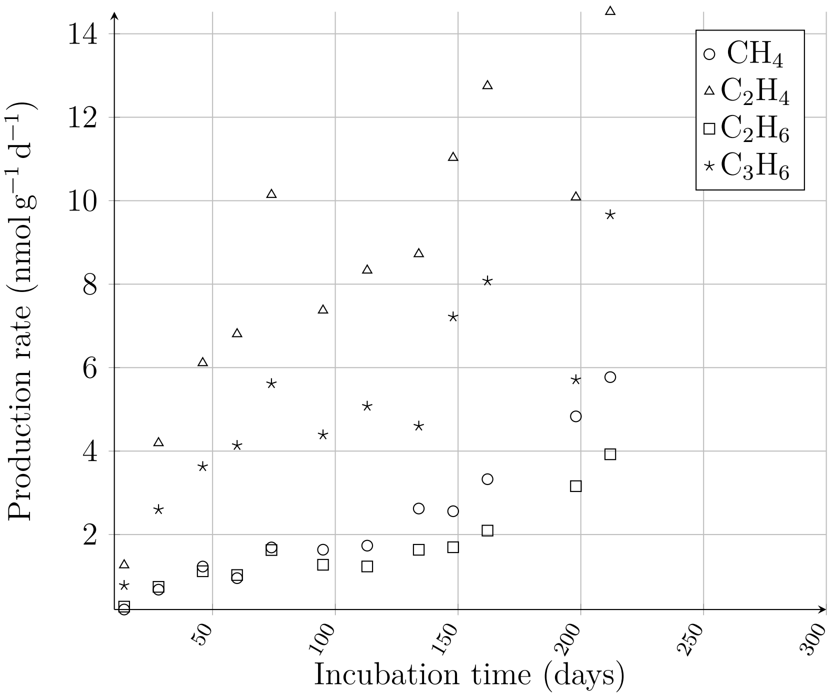

Figure 3.5: Time evolution of principal compounds production rate, starting from virgin Low density PE (Royer et al. 2018).

plastic components, *Sorting facility*, *Landfill, Incineration, Waste water treatment, Soil* (including surface water and ground water), *Freshwater* (drinking water), *Atmosphere, Greenhouse gasses, Long storage in soil*, Drainage basin (called *Ocean*) and *Food*. The complete network is shown in Figure 3.7.

Plastic products node represents the basin of all plastic products and products with plastic components in use.

The graph component containing Sorting facility, Landfill and Incineration includes all the possible processes adopted for plastic waste disposal (in Figure 3.7, these three nodes are represented in orange). These nodes are very important because the edge from Sorting facility to Plastic products represents the recycled fraction of plastic. The Landfill node is not far to be a sink, since the only out-flows are small losses if compared to the quantity that remains in the site at each iteration.

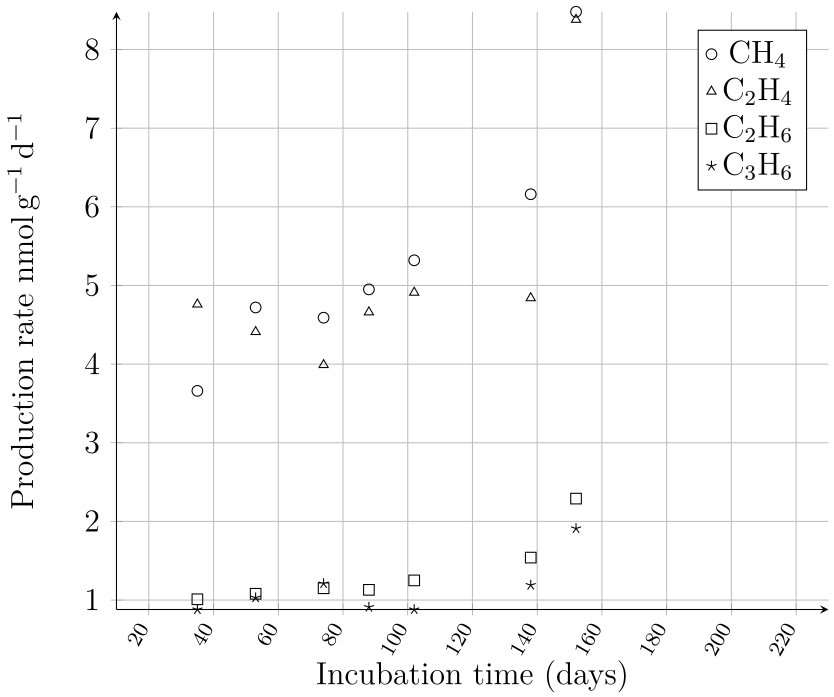

Figure 3.6: Time evolution of principal compounds production rate, starting from Low density PE collected in open ocean (Royer et al. 2018).

Incineration allows the complete transformation of plastic waste in Greenhouse gasses. From there, small losses can reach the atmosphere and soil.

The Waste water treatment node condensed all the processes that take place in water purification (sewers, pre-treatment, sludge and biosolids collection etc.). These processes have been separated from waste treatment since they can affect the Ecosystem not only with small losses, but even directly, e.g. with biosolids application in agriculture.

The Soil vertex include as well the superficial water (basically the watershed until the soil considered as reference) and it is a crucial node for the graph since it is part of many processes mediated by superficial water and atmosphere. In addition, there is a node called Long storage in soil that refers to plastic waste that lays in soil without being transported or transformed. The out-flows from this

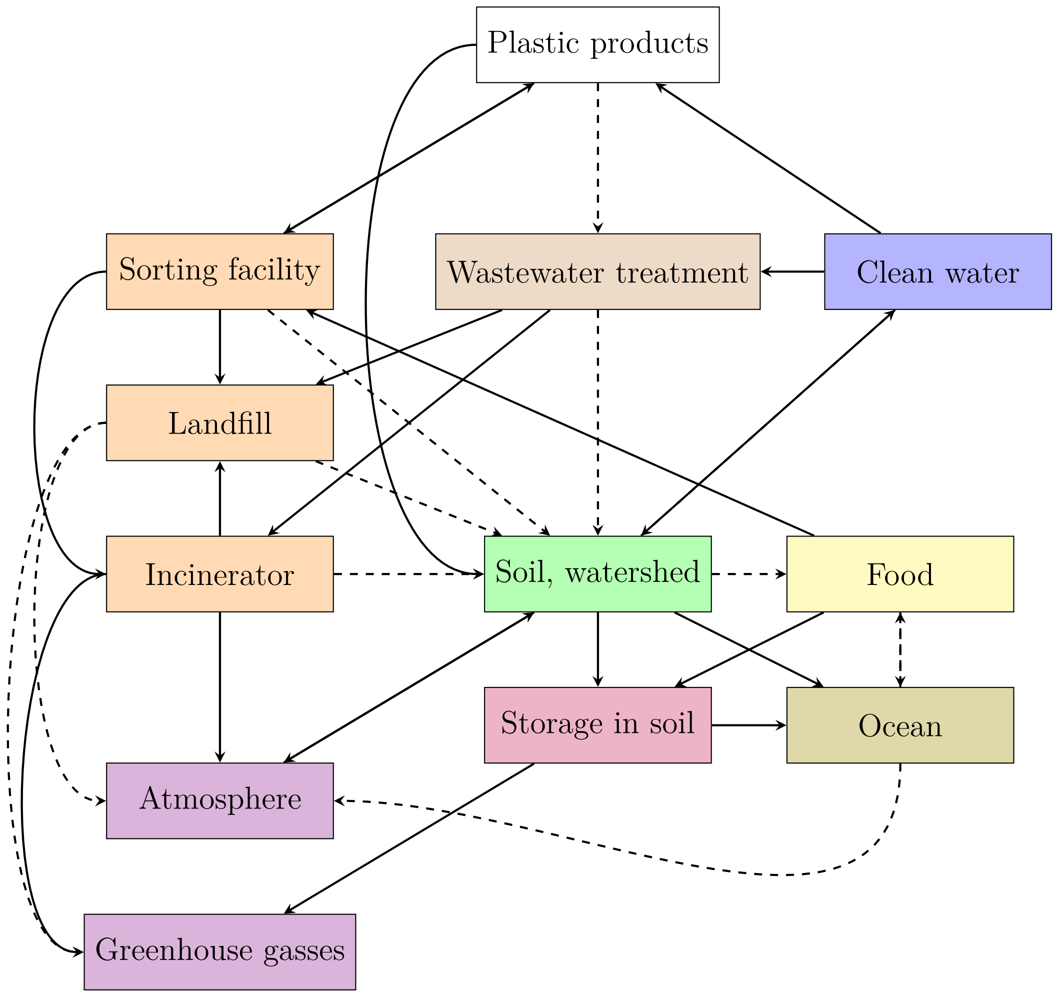

Figure 3.7: Plastic cycle scheme, adapted from (Hoellein et al. 2021). Dashed lines represent small losses with respect to major fluxes indicated by solid lines. Orange boxes are related to solid waste treatment while violet ones to atmosphere.

point are losses towards the Greenhouse gasses and the Ocean.

The Ocean node represents the watershed below the considered soil. The ocean is part of this node ad it represent again a sink-like vertex since only small losses can leave this node as Greenhouse gasses and towards the Food vertex.

The Atmosphere node represent the plastic that lays in the atmosphere in aerial suspension. Here plastic is composed of small debris, micro- and nano-fragments. The Greenhouse gasses vertex is again an atmospheric node and it represents the final fate of plastic. In fact, as anticipated in subsection 3.1.3, plastic degrades in CO_2 and CH_4 gasses, two well known greenhouse gasses (Mann 2022).

The Food node is related to the human food chain and its main out-flows reach the Sorting facility as domestic waste, the Long storage in soil as compost and the Ocean again as losses. Also the drinking water system is considered in this network. It is linked with the aquifer and the Waste water treatment node.

Network representation

According to Figure 3.7, the normalised weight matrix $\boldsymbol{P}$ is:

$$\boldsymbol{P} = \begin{pmatrix} 0.35 & 0.5 & 0 & 0 & 0.05 & 0.1 & 0 & 0 & 0 & 0 & 0 & 0 \\ 0.3 & 0 & 0.449 & 0.25 & 0 & 0.01 & 0 & 0 & 0 & 0 & 0 & 0 \\ 0 & 0 & 0.9 & 0 & 0 & 0.05 & 0 & 0.03 & 0.02 & 0 & 0 & 0 \\ 0 & 0 & 0.05 & 0 & 0 & 0.05 & 0 & 0.15 & 0.75 & 0 & 0 & 0 \\ 0 & 0 & 0.3 & 0.65 & 0 & 0.05 & 0 & 0 & 0 & 0 & 0 & 0 \\ 0 & 0 & 0 & 0 & 0 & 0 & 0.05 & 0.1 & 0 & 0.5 & 0.3 & 0.05 \\ 0.2 & 0 & 0 & 0 & 0.7 & 0.1 & 0 & 0 & 0 & 0 & 0 & 0 \\ 0 & 0 & 0 & 0 & 0 & 0.4 & 0 & 0.6 & 0 & 0 & 0 & 0 \\ 0 & 0 & 0 & 0 & 0 & 0 & 0 & 0 & 1 & 0 & 0 & 0 \\ 0 & 0 & 0 & 0 & 0 & 0 & 0 & 0 & 0.1 & 0.8 & 0.1 & 0 \\ 0 & 0 & 0 & 0 & 0 & 0 & 0 & 0.01 & 0 & 0 & 0.98 & 0.01 \\ 0 & 0.79 & 0 & 0 & 0 & 0 & 0 & 0 & 0 & 0.2 & 0.01 & 0 \end{pmatrix} \tag{3.1}$$

While the representation of the graph is available in Figure 3.8.

Network analysis

In this network, accumulation occurs at: Sorting facility, Landfill, Greenhouse gasses, Storage in soil and Ocean vertices. Their net value respectively are: $\Delta_{\text{Sorting facility}} = 0.290$, $\Delta_{\text{Landfill}} = 0.670$, $\Delta_{\text{Greenhouse gasses}} = 0.870$, $\Delta_{\text{Storage in soil}} = 0.500$ and $\Delta_{\text{Ocean}} = 0.390$.

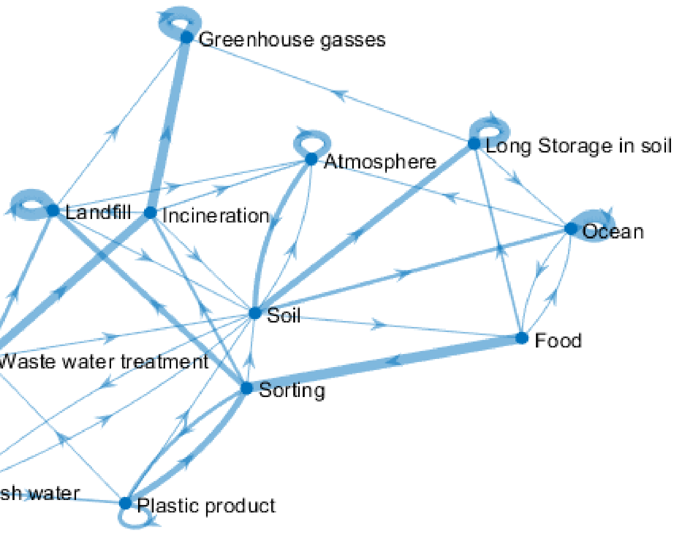

Figure 3.8: Graph representation of plastic cycle.

The accumulation that appears at the waste treatment level (Sorting facility and Landfill vertices) is not so relevant since these nodes are completely artificial and mimic a treatment that is way more complex than that. Furthermore, landfill is by definition an accumulation site so the plastic that arrives there, unfortunately has basically no chance to get out of that, except for being completely transformed in greenhouse gasses in the long term.

However the accumulation in Soil (Storage in soil vertex), in the Ocean and in the atmosphere as greenhouse gasses are the most potentially dangerous ones. Note that, despite the simplicity, this model is capable of finding some general and well known results (e.g the accumulation in the Ocean (Jamali et al. 2021)(Chenillat et al. 2021)), even without precise data supporting it. In addition, as suspected, the network has a sink in the greenhouse gasses vertex. This is correct since some backwards edges, e.g. from methane or carbon dioxide to plastic again, lay in a complete different time scale compared for example to the rate which plastic enters into the Ocean with. For this reason the equilibrium mass distribution is

$$\bar{\boldsymbol{x}} = \begin{pmatrix} 0 & 0 & 0 & 0 & 0 & 0 & 0 & 0 & 1 & 0 & 0 & 0 \end{pmatrix}. \tag{3.2}$$

3.2.1 Robustness analysis

The accumulation appears to be robust in Landfill, in Soil (even if it starts below the accumulation threshold as suggested by the original matrix), in Atmosphere (with very few changes), as Greenhouse gasses, in Long storage in soil (even if with after more than 300 changes, accumulation seems to stop) and in the Ocean (where some changes may reduce the accumulation). Full results are shown in Figures 3.9, 3.10, 3.11, 3.12, 3.13 and 3.14.

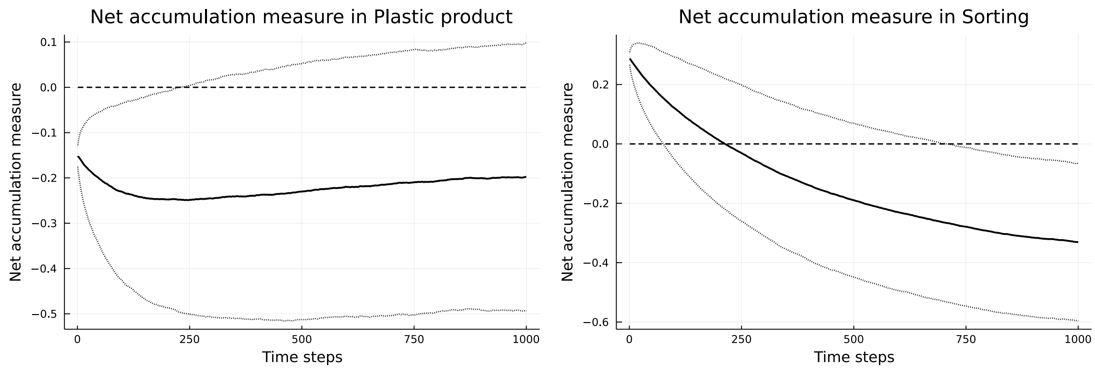

Figure 3.9: Robustness results for Plastic products and Sorting facility. Solid lines represent mean values of simulations, dotted lines the mean values plus and minus the standard deviation and dashed line the net accumulation threshold.

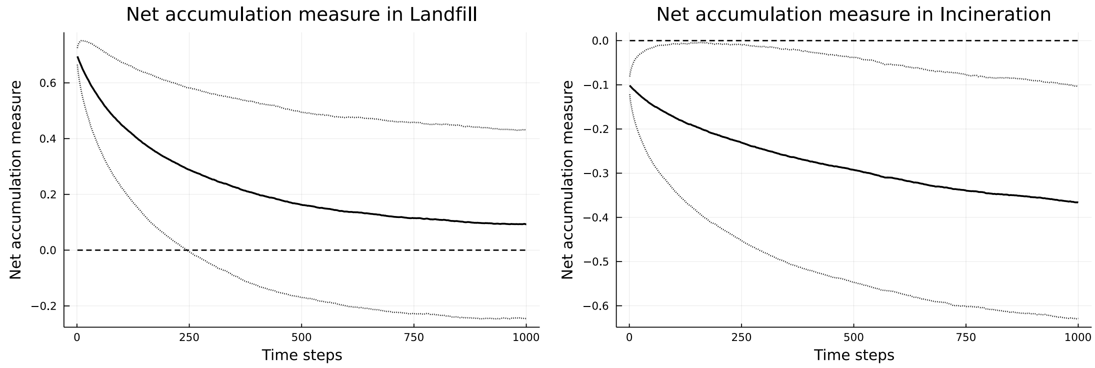

Figure 3.10: Robustness results for accumulation in Landfill and Incineration. Solid lines represent mean values of simulations, dotted lines the mean values plus and minus the standard deviation and dashed line the net accumulation threshold.

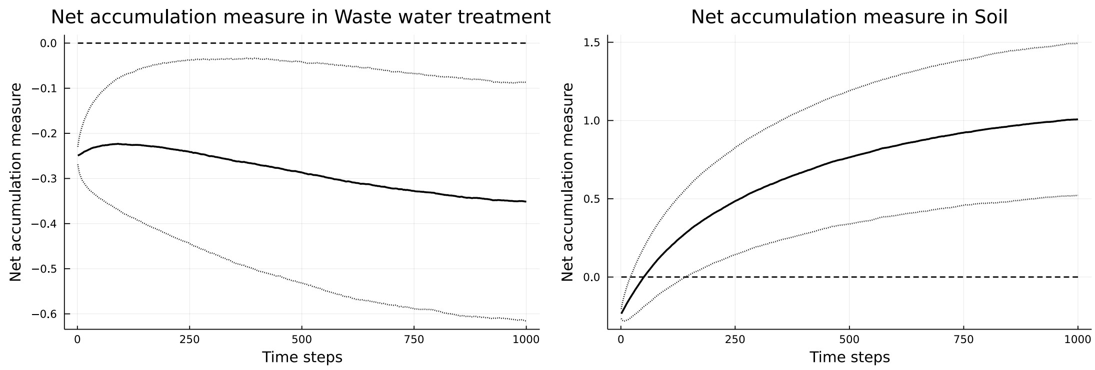

Figure 3.11: Robustness results for accumulation in Wastewater treatment and Soil and watershed. Solid lines represent mean values of simulations, dotted lines the mean values plus and minus the standard deviation and dashed line the net accumulation threshold.

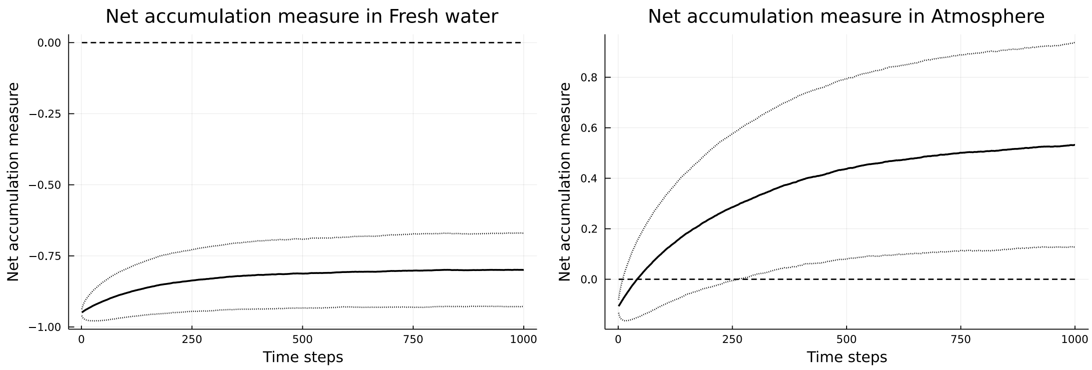

Figure 3.12: Robustness results for accumulation in Clean water and Atmosphere. Solid lines represent mean values of simulations, dotted lines the mean values plus and minus the standard deviation and dashed line the net accumulation threshold.

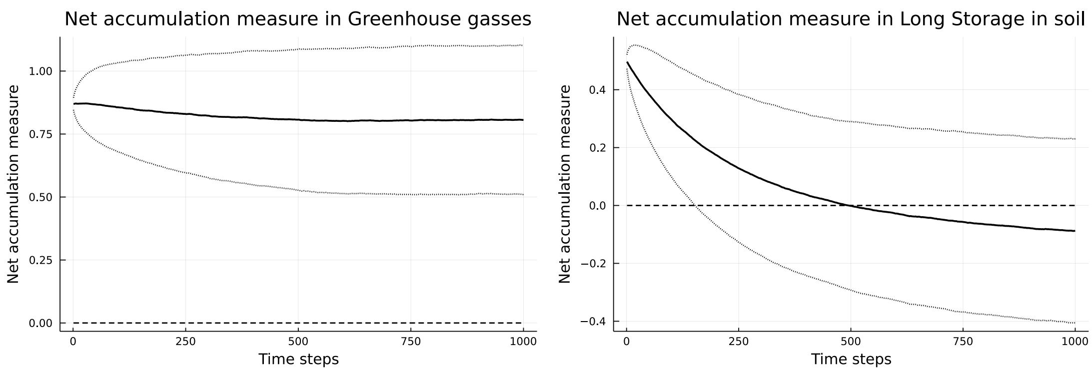

Figure 3.13: Robustness results for accumulation in Atmosphere as greenhouse gasses and Long storage in soil. Solid lines represent mean values of simulations, dotted lines the mean values plus and minus the standard deviation and dashed line the net accumulation threshold.

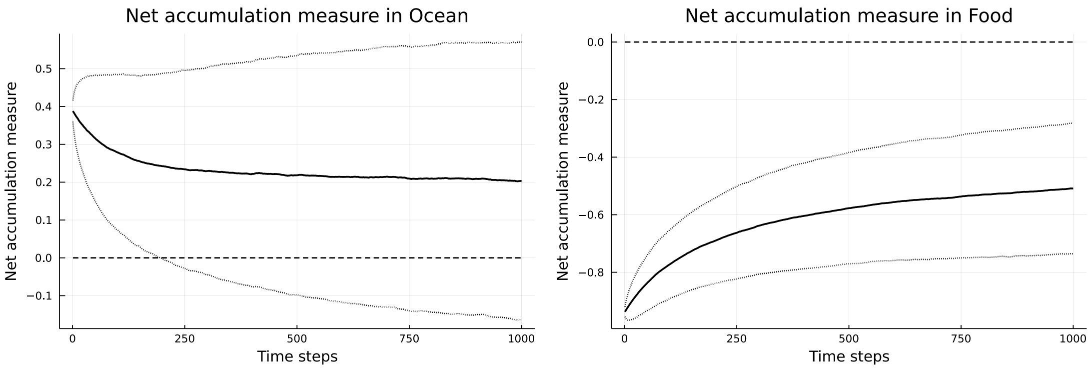

Figure 3.14: Robustness results for accumulation in Ocean and Food. Solid lines represent mean values of simulations, dotted lines the mean values plus and minus the standard deviation and dashed line the net accumulation threshold.

Conclusion

Based on current technology, our world can count on finite resources. This implies that without a significant change of pace, new materials will be everyday more rare and difficult to be extracted. In few words, the linear paradigm of consumption/production is no longer sustainable on the long run (Moriarty et al. 2011). For this reason recycling old materials could at the same time solve both the raw materials procurement and the waste accumulation. However, this new strategy, referred as *Circular economy*, can imply some undesired effects, such as the accumulation of harmful compounds in the environment and in human body, as a direct consequence of circularity.

In the literature circularity has not been investigated with a complex network perspective. So far, plastic and heavy metals cycles have been drawn based on empirical observations and stochastic simulations: (Shi et al. 2018), (Nicholson et al. 2006), (Belon et al. 2012), (Keller et al. 2001) for heavy metals and (Hoellein et al. 2021) and (Windsor et al. 2019) for plastic. In this work, a *Linear network flow dynamics* model is used for providing the identification of potentially dangerous place of accumulation for heavy metals and plastic. In case of heavy metals, based on available data, this approach predicts big accumulation in soil, that is even robust with respect to small perturbations on the network. This is confirmed by previous studies on heavy metals contamination of soil where only compost is used as organic fertiliser (Baldantoni et al. 2010)(Gigliotti et al. 1996)(Jordao et al.

2006). For plastic, according to the model, accumulation happens in soil, ocean and atmosphere as greenhouse gasses, in great accordance with recent studies and observations (Chenillat et al. 2021), (Jamali et al. 2021).

In order to better estimate the accumulation rates, more data are needed both for heavy metals and plastic. Further research should be addressed to evaluate the behaviour of deep soil in terms of adsorption and water runoff as a function of land morphology, weather conditions and crops. For plastic, more research is needed for estimating the volume of network flows. More generally, a greater attention should be payed on the whole recycling process in order to prevent these and other potentially dangerous accumulations.

This work can be considered a starting point for analysing future scenarios with some set target (e.g. increase recycled fraction of plastic, zero waste into landfill[1]). With small changes and according to an energy function, some profitable stochastic paths can be followed change by change, with the purpose of exploring some real policies to be adopted. Finally, the best path can be selected from the bundle, once defined a suitable measure in term of economic cost.

[1]See https://plasticseurope.org/sustainability/circularity/recycling/zero-plastics-to-landfill/

Bibliography

Ahmed, T., M. Shahid, et al. (2018). «Biodegradation of plastics: current scenario and future prospects for environmental safety». In: *Environmental Science and Pollution Research* 25, pp. 7287–7298 (cit. on pp. xi, xiv, 43–45).

Anderson, P. W. (1972). «More is different». In: *Science* 177.4047, pp. 393–396 (cit. on p. 1).

ANPA and P. Paris (2001). *Fertilizzanti commerciali. Aspetti normativi e primi risultati sulla caratterizzazione analitica di alcuni prodotti in commercio*. Tech. rep. 3. Roma: ANPA (cit. on pp. xi, 27, 28).

Appenroth, K. J. (Jan. 2010). «What are "heavy metals" in Plant Sciences?» In: *Acta Physiol Plant* 32, pp. 615–619 (cit. on pp. xii, 21, 22).

ARPA (2019). *Monitoraggio qualità delle acque*. URL: `https://webgis.arpa.piemonte.it/monitoraggio_qualita_acque_mapseries/monitoraggio_qualita_acque_webapp/` (cit. on p. 27).

Badan, L. (2012). *Relazione tecnica sulle deposizioni atmosferiche nel comune di Cerano*. Tech. rep. Torino: Arpa Piemonte (cit. on pp. xi, 27).

Baldantoni, D., A. Leone, P. Iovieno, L. Morra, M. Zaccardelli, and A. Alfani (2010). «Total and available soil trace element concentrations in two Mediterranean agricultural systems treated with municipal waste compost or conventional mineral fertilizers». In: *Chemosphere* 80, pp. 1006–1013 (cit. on pp. v, 35, 56).

Battiston, S., G. Caldarelli, R. M. May, T. Roukny, and J. E. Stiglitz (2016). «The price of complexity in financial networks». In: *Proceedings of the National Academy of Sciences* 113.36, pp. 10031–10036 (cit. on p. 2).

Battiston, S., J. D. Farmer, et al. (2016). «Complexity theory and financial regulation». In: *Science* 351.6275, pp. 818–819 (cit. on pp. 2, 4, 17).

Battiston, S., I. Monasterolo, K. Riahi, and B. J. van Ruijven (2021). «Accounting for finance is key for climate mitigation pathways». In: *Science* 372.6545, pp. 918–920 (cit. on p. 4).

Battiston, S., M. Puliga, R. Kaushik, P. Tasca, and G. Caldarelli (2012). «DebtRank: Too Central to Fail? Financial Networks, the FED and Systemic Risk». In: *Scientific Reports* 2.541 (cit. on p. 2).

Belon, E., M. Boisson, I.Z. Deportes, T.K. Eglin, I. Feix, A.O. Bispo, L. Galsomies, S. Leblond, and C.R. Guellier (Oct. 2012). «An inventory of trace elements inputs to French agricultural soils». In: *Science of the Total Environment* 439, pp. 87–95 (cit. on pp. 7, 56).

Ben-El-Mechaieh, H. and Y. A. Mechaiekh (2022). «An elementary proof of the Brouwer's fixed point theorem». In: *Arabian Journal of Mathematics* 11, pp. 179–188 (cit. on p. 11).

Bengtsson, H., G. Alvenas, S.I. Nilsson, B. Hultman, and I. Oborn (2006). «Cadmium, copper and zinc leaching and surface run-off losses at the Ojebyn farm in Northern Sweden. Temporal and spatial variation». In: *Agriculture, Ecosystems and Environment* 113, pp. 120–138 (cit. on pp. xi, 29).

Bonten, L. T. C., P. F. A. M. Romkens, and D. J. Brus (2008). «Contribution of Heavy Metal Leaching from Agricultural Soils to Surface Water Loads». In: *Environmental Forensics* 9, pp. 252–257 (cit. on pp. xi, 29).

Brizio, P., A. Benedetto, S. Squadrone, A. Curcio, M. Pellegrino, M. Ferrero, and M. C. Abete (2016). «Heavy metals and essential elements in Italian cereals».

In: *Food Additives and Contaminants: Part B* 9.4, pp. 261–267 (cit. on pp. xi, 29).

Caldarelli, G. (2020). «A perspective on complexity and networks science». In: *J. Phys. Complex.* 1.021001, p. 5 (cit. on pp. 1, 2).

— ed. (2010). *Senza uguali.* Milan, Italy: Egea (cit. on p. 3).

Chenillat, F., T. Huck, C. Maes, N. Grima, and B. Blanke (2021). «Fate of floating plastic debris released along the coasts in a global ocean model». In: *Marine Pollution Bulletin* 165, pp. 112–116 (cit. on pp. v, 7, 51, 57).

Como, G. and F. Fagnani (Dec. 2021). *Lecture notes on Network Dynamics* (cit. on p. 7).

Database, The World Bank (2018a). *Cereal yield (kg per hectare) - Italy.* URL: `https://data.worldbank.org/indicator/AG.YLD.CREL.KG?locations=IT` (cit. on p. 28).

— (2018b). *Fertilizer consumption (kilograms per hectare of arable land) - Italy.* URL: `https://data.worldbank.org/indicator/AG.CON.FERT.ZS?locations=IT` (cit. on p. 27).

Donati, F., G. A. Aguilar-Hernandez, C. P. Sigüenza-Sánchez, A. de Koning, J. F. D. Rodrigues, and A. Tukker (2020). «Modeling the circular economy in environmentally extended input-output tables: Methods, software and case study». In: *Resources, Conservation and Recycling* 152, p. 104508 (cit. on p. 17).

Dube, A., R. Zbytniewski, T. Kowalkowski, E. Cukrowska, and B. Buszewski (2001). «Adsorption and Migration of Heavy Metals in Soil». In: *Polish Journal of Environmental Studies* 10.1, pp. 1–10 (cit. on pp. 24, 29).

Duffus, J. H. (2002). «"Heavy metals"—a meaningless term?» In: *Pure Appl. Chem.* 74.09/2020, pp. 793–807 (cit. on pp. 20, 21).

Eriksen, M., L. C. M. Lebreton, et al. (Dec. 2014). «Plastic Pollution in the World's Oceans: More than 5 Trillion Plastic Pieces Weighing over 250,000 Tons Afloat at Sea». In: *PLOS ONE* 9.12, pp. 1–15. DOI: 10.1371/journal.pone.0111913 (cit. on p. 7).

Gerdol, R., L. Bragazza, et al. (2000). «Monitoring of heavy metal deposition in Northern Italy by moss analysis». In: *Environmental Pollution* 108, pp. 201–208 (cit. on pp. 26, 27).

Gewert, B., M. M. Plassmann, and M. MacLeod (2015). «Pathways for degradation of plastic polymers floating in the marine environment». In: *Environmental Science: Processes and Impacts* 17, pp. 1513–1521 (cit. on pp. 39, 40, 42, 44).

Geyer, R., J. R. Jambeck, and K. L. Law (2017). «Production, use, and fate of all plastics ever made». In: *Science Advances* 3, pp. 1–5 (cit. on pp. xiii, 41, 42, 45, 46).

Gigliotti, G., D. Businelli, and P. L. Giusquiani (1996). «Trace metals uptake and distribution in corn plants grown on a 6-year urban waste compost amended soil». In: *Agriculture, Ecosystems and Environment* 58, pp. 199–206 (cit. on pp. v, 35, 56).

Glattfelder, J. B. and S. Battiston (2013). «Backbone of Complex Networks of Corporations: The Flow of Control». In: *Decoding Complexity: Uncovering Patterns in Economic Networks*. Berlin, Heidelberg: Springer, pp. 67–93 (cit. on p. 2).

Hahladakis, J. N., C. A. Velis, R. Weber, E. Iacovidou, and P. Purnell (2018). «An overview of chemical additives present in plastics: Migration, release, fate and environmental impact during their use, disposal and recycling». In: *Journal of Hazardous Materials* 344, pp. 179–199 (cit. on pp. 44, 46).

Heavy metal emissions in Europe (Nov. 2021). European Environment Agency. URL: https://www.eea.europa.eu/ims/heavy-metal-emissions-in-europe (cit. on p. 23).

Hoellein, T. J. and C. M. Rochman (2021). «The "plastic cycle": a watershed-scale model of plastic pools and fluxes». In: *Front Ecol Environ* 19.3, pp. 176–183 (cit. on pp. iv, xiv, 7, 17, 46, 49, 56).

Institute, Science Hystory (2022). *History and Future of Plastics.* URL: `https://www.sciencehistory.org/the-history-and-future-of-plastics` (cit. on p. 40).

Jacquez, J. A. and C. P. Simon (1993). «Qualitative theory of compartmental systems». In: *SIAM Review* 35.1, pp. 43–79 (cit. on p. 8).

Jaishankar, M., T. Tseten, N. Anbalagan, B. B. Mathew, and K. N. Beeregowda (Nov. 2014). «Toxicity, mechanism and health effects of some heavy metals». In: *Interdiscip Toxicol.* 7.2, pp. 60–72 (cit. on pp. 21, 22).

Jamali, A. and M. Mahdianpari (2021). «A Cloud-Based Framework for Large-Scale Monitoring of Ocean Plastics Using Multi-Spectral Satellite Imagery and Generative Adversarial Network». In: *Water* 13.18 (cit. on pp. v, 7, 51, 57).

Jambeck, J. R., R. Geyer, C. Wilcox, T. R. Siegler, M. Perryman, A. Andrady, R. Narayan, and K. Lavender Law (2015). «Plastic waste inputs from land into the ocean». In: *Science* 347.6223, pp. 768–771 (cit. on p. 40).

Jarup, L. (Dec. 2003). «Hazards of heavy metal contamination». In: *Br Med Bull.* 68.1, pp. 167–182 (cit. on p. 22).

Jordao, C. P., C. C. Nascentes, P. R. Cecon, R. L. Fontes, and J. L. Pereira (2006). «Heavy metal availability in soil amended with composted urban solid waste». In: *Environmental Monitoring and Assessment* 112, pp. 309–326 (cit. on pp. v, 35, 56).

Keller, A., B. von Steiger, S. E. A. T. M. van der Zee, and R. Schulin (Nov. 2001). «A Stochastic Empirical Model for Regional Heavy-Metal Balances in Agroecosystems». In: *J. Environ. Qual.* 30, pp. 1976–1989 (cit. on pp. xi, 7, 24, 29, 56).

Kim, J. and T. Willhelm (2008). «What is a complex graph». In: *Physica A* 387, pp. 2637–2652 (cit. on p. 2).

Koelmans, B. and S. Pahl (Jan. 2019). *A Scientific Perspective on Microplastics in Nature and Society*. Tech. rep. 09/2020. Berlin, Germany: SAPEA (cit. on pp. 7, 42, 46).

Lopes, C., M. Herva, A. Franco-Uria, and E. Roca (2011). «Inventory of heavy metal content in organic waste applied as fertilizer in agriculture: evaluating the risk of transfer into the food chain». In: *Environ Sci Pollut Res* 18, pp. 918–939 (cit. on p. 24).

Makuch, A. et al. (2022). *The-Russian-invasion-of-Ukraine*. URL: `https://www.britannica.com/place/Ukraine/The-Russian-invasion-of-Ukraine` (cit. on p. 3).

Mann, M. E. (Sept. 2022). *Greenhouse gasses*. URL: `https://www.britannica.com/science/greenhouse-gas` (cit. on p. 50).

Morais, S., F. G. Costa, and M. L. Pereira (2012). «Heavy metals and human health». In: *Environmental health – emerging issues and practice*, pp. 227–246 (cit. on p. 22).

Moriarty, P. and D. Honnery (2011). «Earth's Resources Are Finite». In: *Rise and Fall of the Carbon Civilisation: Resolving Global Environmental and Resource Problems*. London: Springer London, pp. 37–58 (cit. on p. 56).

Nicholson, F. A., S. R. Smith, B. J. Alloway, C. Carlton-Smith, and B. J. Chambers (June 2006). «Quantifying heavy metal inputs to agricultural soils in England and Wales». In: *Water and Environment Journal* 20.2, pp. 87–95 (cit. on pp. 7, 56).

OECD (Feb. 2022). *Global Plastics Outlook: Economic Drivers, Environmental Impacts and Policy Options*. URL: `https://www.oecd-ilibrary.org/sites/`

`f9c3a6c4-en/index.html?itemId=/content/component/f9c3a6c4-en` (cit. on p. 46).

Ortiz, A. Gonzales, C. Guerreiro, and J. Soares (2020). *Air quality in Europe — 2020 report*. Tech. rep. 09/2020. Kongens Nytorv 6, 1050 Copenhagen K, Denmark: European Environment Agency (cit. on pp. xii, 22, 23).

Page, J., D. Hinshaw, and B. McKay (2021). «In Hunt for Covid-19 Origin, Patient Zero Points to Second Wuhan Market». In: *The Wall Street Journal* (cit. on p. 3).

Peng, C., M. Wang, and W. Chen (May 2016). «Modelling cadmium contamination in paddy soils under long-term remediation measures: Model development and stochastic simulations». In: *Environmental Pollution* 216, pp. 146–155 (cit. on p. 7).

Ritchie, H. and M. Roser (2018). «Plastic Pollution». In: *Our World in Data*. https://ourworldindata.org/plastic-pollution (cit. on pp. xiii, 41, 43, 46).

Rodriguez, F. (2022). *Plastic*. URL: `https://www.britannica.com/science/plastic` (cit. on p. 39).

Roser, M., H. Ritchie, and E. Ortiz-Ospina (2013). «World Population Growth». In: *Our World in Data*. https://ourworldindata.org/world-population-growth (cit. on pp. xii, 4).

Rossi, R. (Dec. 2019). *Irrigation in EU agriculture*. Tech. rep. PE 644.216. European Parliament (cit. on p. 27).

Royer, S. J., S. Ferron, S. T. Wilson, and D. M. Karl (2018). «Production of methane and ethylene from plastic in the environment». In: 13.8, pp. 1–13 (cit. on pp. xi, xiv, 44, 46–48).

Sangiumsak, N. and P. Punrattanasin (2014). «Adsorption Behavior of Heavy Metals on Various Soils». In: *Polish Journal of Environmental Studies* 23.3, pp. 853–865 (cit. on p. 29).

Shi, T., J. Mab, X. Wub, T. Jub, X. Linb, Y. Zhangb, X. Lib, Y. Gongb, and Fuyong Wu Hong Houb Long Zhaob (Aug. 2018). «Inventories of heavy metal inputs and outputs to and from agricultural soils: A review». In: *Ecotoxicology and Environmental Safety* 164, pp. 118–124 (cit. on pp. iv, 7, 16, 24, 25, 56).

Smith, P., D. Reay, and J. Smith (2021). «Agricultural methane emissions and the potential formitigation». In: *Philosophical Transactions of the Royal Society A* 379, pp. 7287–7298 (cit. on p. 45).

Stadler, K. et al. (2018). «EXIOBASE 3: Developing a Time Series of Detailed Environmentally Extended Multi-Regional Input-Output Tables». In: *Journal of Industrial Ecology* 22.3, pp. 502–515 (cit. on pp. 4, 17).

Stringer, R. and P. Johnston, eds. (2001). *Chlorine and the environment: an overview of the chlorine industry*. Dordrecht, The Netherlands: Kluwer Academic Publishers (cit. on p. 44).

Take Action for the Sustainable Development Goals (n.d.). UN. URL: `https://www.un.org/sustainabledevelopment/sustainable-development-goals/` (cit. on p. 3).

Tran, M. (2014). «Modeling Sustainability Transitions on Complex Networks». In: *Wiley Periodicals* 19.5, pp. 8–22 (cit. on pp. 4, 5).

UN (2022). *Sustainable Development Goals*. URL: `https://www.undp.org/sustainable-development-goals` (cit. on p. 4).

Vargas-Solano, S. V., F. Rodríguez-González, R. Martínez-Velarde, S. S. Morales-García, and M. P. Jonathan (2022). «Removal of heavy metals present in water from the Yautepec River Morelos México, using Opuntia ficus-indica mucilage». In: *Environmental Advances* 7, p. 100160 (cit. on p. 32).

Velde, K. Van de, C. F. Boutron, et al. (2000a). «A two hundred years record of atmospheric Cadmium, Copper and Zinc concentrations in high altitude snow and ice from the French-Italian Alps». In: *Geophysical Research Letters* 27.2, pp. 249–252 (cit. on p. 27).

Velde, K. Van de, C. F. Boutron, C. P. Ferrari, A. L. Moreau, R. J. Delmas, C. Barbante, T. Bellomi, G. Capodaglio, and P. Cescon (Jan. 2000b). «A two hundred years record of atmospheric Cadmium, Copper and Zinc concentrations in high altitude snow and ice from the French-Italian Alps». In: *Geophysical research letters* 27, pp. 249–252 (cit. on p. 23).

Vitali, S., J. B. Glattfelder, and S. Battiston (Oct. 2011). «The Network of Global Corporate Control». In: *PLoS ONE* 6.12 (cit. on p. 2).

Williams, M., ed. (2010). *Uncontrolled Risk: Lessons of Lehman Brothers and How Systemic Risk Can Still Bring Down the World Financial System*. McGraw Hill (cit. on p. 3).

Windsor, F. M., I. Durance, A. A. Horton, R. C. Thompson, C. R. Tyler, and S. J. Ormerod (2019). «A catchment-scale perspective of plastic pollution». In: *Global Change Biology* 25, pp. 1207–1221 (cit. on pp. iv, 7, 17, 40, 46, 56).

Wriedt, G., M. Van der Velde, A. Aloe, and F. Bouraoui (2008). *Water Requirements for Irrigation in the European Union*. Tech. rep. JRC 46748. Ispra (VA): EU Commission, Joint Research Centre (cit. on p. 27).